ANL-6649

Argonne National Laboratory

FABRICATION OF UO_2-STAINLESS STEEL DISPERSION FUEL FOR BORAX-V NUCLEAR SUPERHEAT

by

W. C. Kramer and C. H. Bean

ANL-6649
Metals, Ceramics,
and Materials
(TID-4500, 28th Ed.)
AEC Research and
Development Report

ARGONNE NATIONAL LABORATORY
9700 South Cass Avenue
Argonne, Illinois 60440

FABRICATION OF UO_2-STAINLESS STEEL DISPERSION FUEL FOR BORAX-V NUCLEAR SUPERHEAT

by

W. C. Kramer and C. H. Bean

December 1963

Metallurgy Division
Program 7.6.14

Final Report

A portion of the material contained in this report has been reported in the following Metallurgy Division Reports:

ANL-6330, pp. 74-77
ANL-6516, pp. 82-91
ANL-6677, pp. 69-74

Operated by The University of Chicago
under
Contract W-31-109-eng-38
with the
U. S. Atomic Energy Commission

TABLE OF CONTENTS

LIST OF FIGURES

LIST OF FIGURES

LIST OF FIGURES

LIST OF TABLES

FABRICATION OF UO_2-STAINLESS STEEL DISPERSION FUEL FOR BORAX-V NUCLEAR SUPERHEAT

by

W. C. Kramer and C. H. Bean

ABSTRACT

The superheat section of the Fifth Boiling Reactor Experiment (BORAX-V) is fueled with enriched uranium (93 w/o U^{235}) in the form of UO_2 in a matrix of stainless steel.[1] Stainless steel-clad plates containing the fuel were fabricated by the Atomics International Division of North American Aviation in accordance with Material Processing Contract No. 31-109-38-1252, dated October 3, 1960, and Supplemental Agreement No. 1 thereto, dated June 22, 1961.

This report describes the nondestructive and destructive evaluation of fuel plates at ANL, the development and evaluation of procedures for assembly of fuel plates, the evaluation of fuel subassemblies, and the assembly of fuel element components. A total of 700 fuel plates were used in fabricating the 175 brazed subassemblies needed to complete 35 BORAX-V Superheat Fuel Elements.

INTRODUCTION

The fuel for the superheater of BORAX-V is of a UO_2-stainless steel cermet type similar to fuel developed for use in pressurized water reactors[2,3] and organic-moderated reactors.[4] Selection of a previously developed type of fuel offered the economic advantages of commercial availability and relative ease of delivery. With the exception of overall plate dimensions and variations in the weight percent of UO_2 in the core these plates closely resemble those developed by Atomics International for the OMRE. The overall dimensional tolerances for the finished plates and plate cores are shown in Table I.

The fuel was designed for service in steam at 42.2 kg/cm^2 gage (600 psig) with a maximum fuel-surface temperature of 650°C. The design average heat flux is 8.294 cal/cm^2-sec with a maximum flux estimated at 17.568 cal/cm^2-sec. The design fuel-center temperature is 670°C.[1]

Table I

PLATE DIMENSIONS OF BORAX-V SUPERHEAT FUEL

	Length, cm (in.)	Width, cm (in.)	Thickness, cm (in.)
Plate	64.14 ± 0.01 (25.250 ± 0.005)	9.309 ± 0.005 (3.665 ± 0.002)	0.074/0.079 (0.029/0.031)
Core	60.96 ± 1.91 (24.000 ± 0.750)	8.88 ± 0.13 (3.495 ± 0.052)	0.033/0.038 (0.013/0.015)
End Cladding	0.64 (0.250) min		
Side Cladding		0.22 ± 0.06 (0.085 ± 0.025)	
Face Cladding			0.018 (0.007) min

Two separate superheat loadings were fabricated. One loading will be positioned in the central part of the reactor core with boiling fuel surrounding the superheat fuel. After operation with this core configuration, the central elements will be removed, the boiling core will be relocated to the central position, and the other superheat loading will be placed in peripheral element positions.

A superheat fuel element is made of five subassemblies of fuel plates with intervening water gaps. Each subassembly contains four fuel plates separated by 1.59-mm (0.062-in.) steam channels. The design criteria dictated the use of plates containing four different amounts of UO_2. Peripheral elements contain more oxide than elements to be located in the central part of the reactor core. In addition, the two outside plates in each subassembly contain only about half as much fuel as the two inside plates. This enables the design heat flux and operating temperatures to be most economically attained.

A lettering system was devised to differentiate between the four plate types. Plates in peripheral elements are Full Peripheral Enriched (FPE) and Half Peripheral Enriched (HPE). Plates in central elements are Full Central Enriched (FCE) and Half Central Enriched (HCE). Depending on subassembly position, each plate is either full (FPE or FCE) or half (HPE or HCE) loaded. The four different amounts of UO_2 contained in the plates are given in Table II.

The width-to-thickness ratio in the BORAX-V plates (>100:1) required the use of spacers between plates in addition to the rigid support provided at the plate edges. Development work was necessary to determine the type of spacer to use and the method of fastening the spacers to the plates. Vacuum-furnace brazing was chosen rather than mechanical fastening or welding to secure the plates, spacers, and side plates in correct subassembly configuration.

Table II

COMPOSITION OF CORE IN BORAX-V SUPERHEAT FUEL PLATES

Type of Fuel Plate	Core Composition		Contained UO_2 (g)	Contained U(w/o)
	w/o UO_2	w/o 304-B SS		
Half Central	11.52	88.48	18.3	10.16
Full Central	21.17	78.83	34.1	18.67
Half Peripheral	18.02	81.98	28.9	15.89
Full Peripheral	32.26	67.74	54.0	28.45

The brazed subassemblies were inserted in welded stainless steel insulating cans. Five insulated subassemblies welded with the flow vanes, riser, and nozzle constitute a fuel element. This final portion of the assembly was straightforward and required no particular development.

FABRICATION OF FUEL PLATES

Several commerical fabricators had experience in the manufacture of dispersion-type fuel. A specification was prepared specifying raw material and final product qualities for the superheater fuel plates. Material processing contract No. 31-109-38-1252 was awarded to Atomics International (AI) Division, North American Aviation, on October 3, 1960, for the fabrication of the fuel plates. Appendix B of this contract includes the specifications and drawing that the fabricated fuel plates were to fulfill. The specifications and the fuel-plate drawing are part of Appendix A of this report. Supplemental Agreement No. 1 to this contract, effective June 22, 1961, is also included in Appendix A.

Fabrication of the plates involved the blending of high-fired UO_2 particles with austenitic stainless steel powder; pressing, sintering, and coining the core blanks; welding the cores into stainless steel frames and cover plates; hot rolling and cold finishing the welded compacts.

Prior to the fabrication of production fuel plates, 48 plates, 12 of each type, containing depleted uranium (0.22 w/o U^{235}) in the form of UO_2, were made for evaluation of fuel plate-fabrication procedures. Twenty-four of these plates were evaluated at AI and 24 at ANL. After acceptance by the Laboratory of the depleted evaluation plates, an additional 160 depleted plates were fabricated. These depleted plates were used for development of fuel-element-assembly procedures. After completion of the fabrication of all depleted plates, a total of 840 fuel plates containing enriched

uranium were fabricated, of which 16 were sectioned for destructive testing and evaluation at AI. Of the 824 enriched plates remaining, 700 were assembled into elements for use in BORAX-V.

Raw Materials

The core material of the fuel plates consisted of a dispersion of UO_2 particles in austenitic stainless steel (SS). A dense, high-fired type of oxide was used rather than a fused type because it affords greater resistance to fragmentation and stringering during fabrication.(2) It therefore provides the optimum dispersion of discrete oxide particles. Since little or no irradiation or fuel-performance data were available pertaining to spherical oxide, there was no justification for specifying this particular type.

The particle size range was set at 37 to 88μ because of the following considerations: In the particular dispersion system used for the BORAX-V superheat fuel, the fissile phase (UO_2) is mechanically weaker than the non-fissile matrix (304-B SS). Therefore, an increase in the average size of the fissile particles would tend to concentrate the weaker phase of the core and result in a fuel plate of lower strength. Heat transfer from larger particles is also not as efficient as from smaller particles. The tendency of fissile particles to agglomerate during fabrication increases as the particle size decreases.(5) Experience has shown that the matrix-metal particles should be smaller than the fissile particles to achieve good homogeneity and to avoid excessive agglomeration of the fissile particles.(2) Since a damaged zone of constant thickness produced by fission products recoiling into a specific matrix will surround each fissile particle, reduction of particle size increases the fraction of damaged matrix. The best combination of heat-transfer and mechanical properties both before and after irradiation is therefore achieved by using particles within a limited size range which is thought to be the one selected.

An AISI Type 304-L stainless steel was specified for cladding components and Type 304-B in powder form, as the plate core matrix material. The maximum carbon content for both the 304-L and 304-B stainless steels was specified as 0.03 w/o. Use of low-carbon austenitic stainless steel minimizes susceptibility to grain-boundary carbide precipitation and subsequent intergranular corrosion.(6) Type 304-B stainless steel also has 2.5 w/o Si to improve the mechanical properties (hardness and strength) of the plate cores.(7)

Plate Qualities*

Plate, core, and cladding dimensions have been given in Table I. Adequate containment of fissionable material was ensured by specifying

*Detailed specifications are given in Appendix B, pp. 63-74.

the limiting dimensions of the end, side, and face cladding. Core length was also specified, and each plate was marked to indicate whether the core was over or under 61 cm (24 in.) in length.

Plate squareness, flatness, and straightness were specified to facilitate the assembly operations. Bright annealing of finished plates was required to flatten the plates and to minimize distortion during subsequent heating for assembly brazing. A fine surface finish was necessary to reduce steam erosion during reactor operation. Elimination of radioactive surface contamination was also necessary to prevent transfer of any such contamination to the coolant steam. Control of halide ion concentration in the superheat core is important to minimize the probability of stress corrosion of the stainless steel.

In a true dispersion fuel, fissile particles remain surrounded by a continuous matrix of material that is not damaged by fission products during reactor operation.[2] There is, however, an annular volume of matrix material surrounding each UO_2 particle into which fission products recoil. If discrete particles are homogeneously dispersed, there will remain a continuous unaffected matrix. Plates with this unaffected matrix will display more favorable mechanical and physical properties than uniformly affected material, whereas oxide stringers and particle groups tend to concentrate mechanical weakness, radiation damage, and heat production. For this reason, necessary requirements for homogeneity of oxide dispersion, lengths of oxide stringers, and grouping of oxide particles were specified (see Appendix B of the contract in Appendix A of this report). Other advantages of a homogeneous core are a uniform hot zone and a plate with uniform mechanical properties.

The presence of nonbonded areas or inclusions between core and cladding would seriously hinder heat transfer at these points and cause hot spots on the plate. The bond requirment was specified as in Appendix B of the contract. It was also specified that cladding mating surfaces should be integrally bonded, because cladding-bond failure could lead to exposure of plate cores and ultimately to radioactive contamination of the reactor steam system.

EVALUATION OF FUEL PLATES

As detailed in Appendix A, the contract required that 208 depleted fuel plates and 840 enriched fuel plates be fabricated according to ANL specifications. The fuel plates were used as follows:

1. Six of each of the four types (see Table II) of depleted plates were fabricated and thoroughly examined and tested, both nondestructively and destructively. The results of the examination of these plates were

used to evaluate the fabrication procedures. When these original depleted plates, or their replacements, were considered satisfactory, all remaining depleted and enriched plates were fabricated with no subsequent changes in production procedures.

2. Forty of each of the four types of depleted plates were fabricated and thoroughly examined and nondestructively tested. These plates, or acceptable replacements, were used to develop assembly procedures. Sufficient completed fuel subassemblies were destructively evaluated so that assembly of enriched fuel plates could proceed with a high degree of confidence in the assembly procedures.

3. The 840 enriched plates, 190 of each of the central types and 230 of each of the peripheral types, were fabricated and thoroughly examined and nondestructively tested. These plates, or acceptable replacements, were brazed into fuel subassemblies and the subassemblies welded into fuel elements for fueling the BORAX-V superheater.

Nondestructive Evaluation

The nondestructive evaluation of fuel plates received from the contractor followed the steps shown in Figure 1.

After the plates had been visually inspected for the presence of pits, dents, scratches, or any other abnormal condition, the weight of each plate was determined to 0.1 g on a Mettler pan balance. The thickness at nine locations on each plate was measured with a one-inch micrometer.

Plate length, width, and squareness were simultaneously measured, with a specially fabricated holding fixture and dial indicator gages, as illustrated in Figure 2. The plate to be measured was set into the holder so that two sides were contiguous to the fixture parts representing the legs of a true 90° angle. The dial indicators were preset to read zero at nominal plate length and width. By moving the indicators from side to side along one end, and from end to end along one side, the deviations from length and width as well as total indicator runout (TIR) were measured to within 0.01 mm (0.0005 in.).

For the measurement of flatness, the edges of each plate were weighted to a surface plate. An 18.2-kg (40-lb) "picture frame" formed with lead-filled iron channels was used to weight the plate edges. The exposed plate surface was then scanned, as shown in Figure 3, with a dial indicator to determine total indicator runout (TIR) each 7.6-cm (3-in.) length to within 0.01 mm (0.0005 in.).

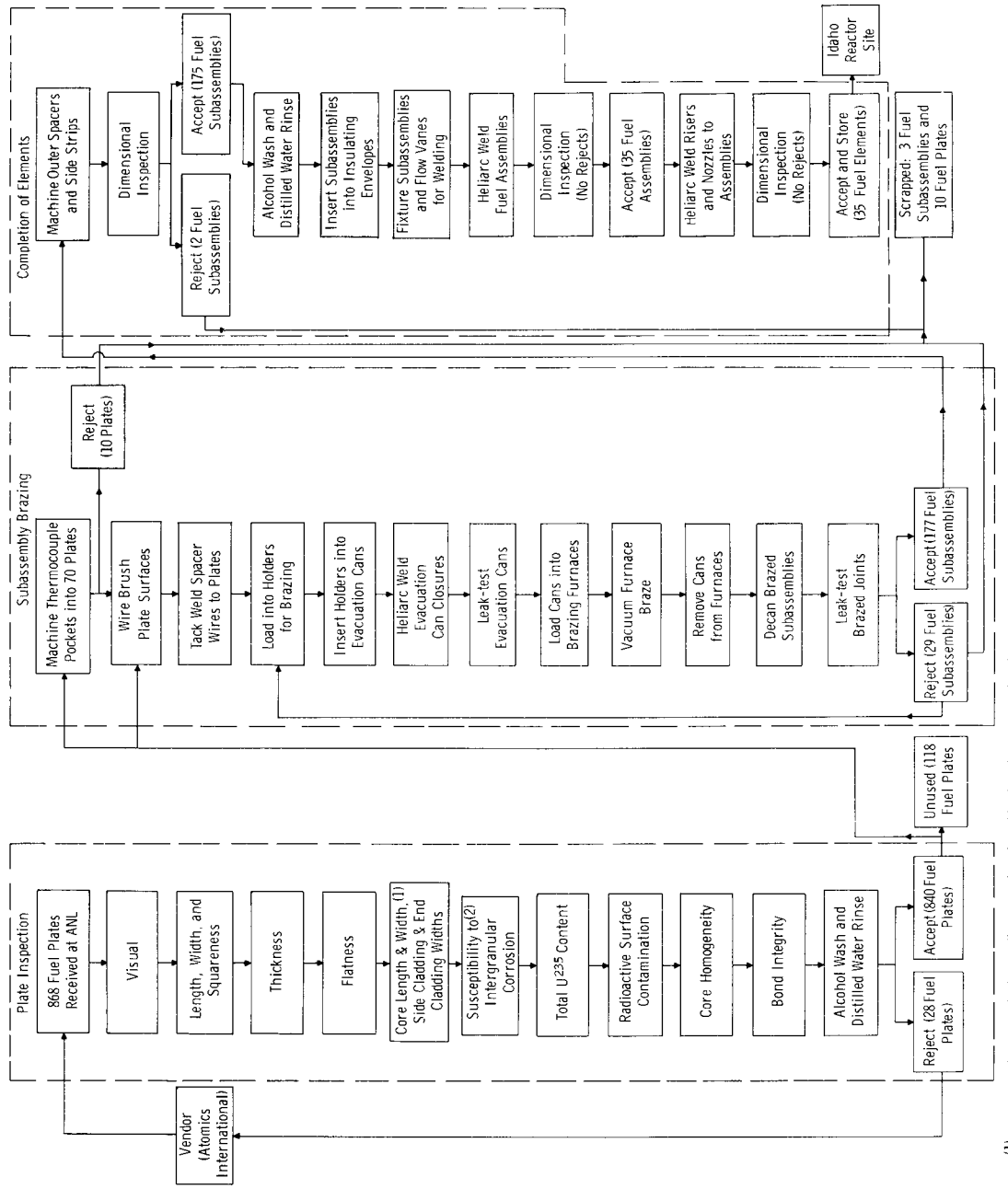

(1)As measured from fuel-plate radiographs furnished by Atomics International.

(2)As determined by Strauss tests performed on a random 10% sample of fuel plate end cladding coupons furnished by Atomics International.

Figure 1. BORAX-V Superheat Fuel-fabrication Flowsheet

Figure 2. Measurement of Fuel-plate Length, Width, and Squareness

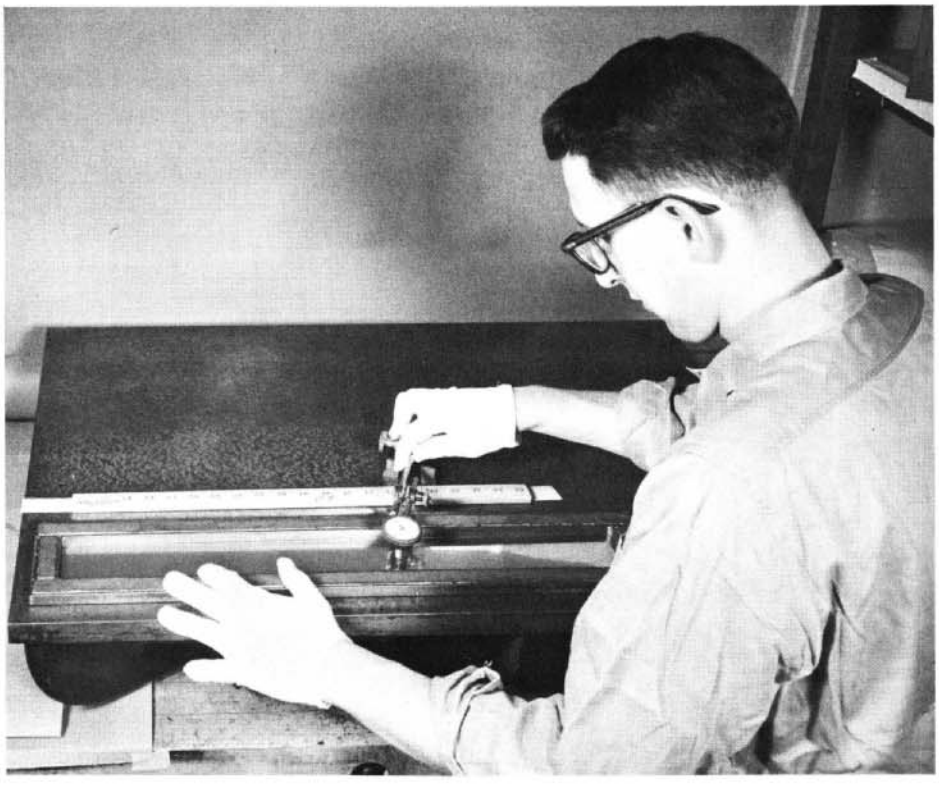

Figure 3. Measurement of Fuel-plate Flatness

Along with each plate, the fabricator was required to furnish a full-plate radiograph. By means of these, core locations were determined and cladding measurements were made as demonstrated in Figure 4. The cladding was measured along both sides at a minimum of four locations.

In addition, each side was scanned rapidly, and the maximum and minimum readings were noted. The measurements, taken with an optical comparator, were accurate to within ±0.1 mm (0.005 in.). Core width was calculated by subtracting side cladding widths from nominal plate widths.

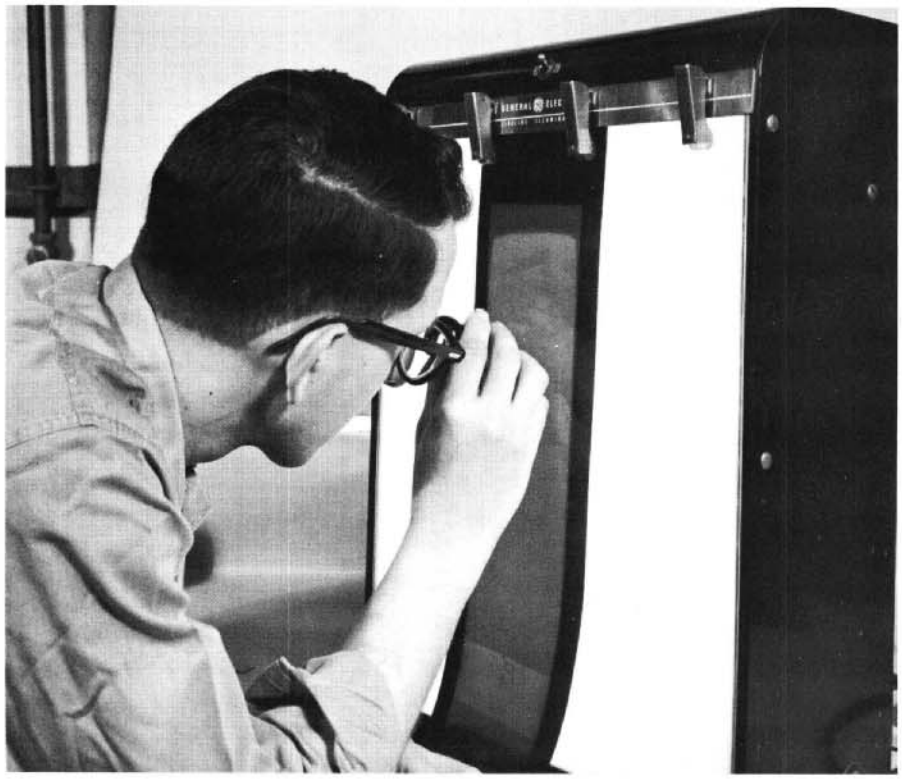

Figure 4. Determination of Fuel-plate Core Location

Maximum and minimum values of the end cladding were measured with a scale to within ±6.4 mm (0.25 in.). The maximum and minimum core lengths were then calculated by subtracting, respectively, minimum and maximum values of the end cladding from the nominal plate length.

Ultrasonic through-transmission testing was used to measure bond integrity within the fuel plates.[8] Lucite holders were used during testing to hold the plates in a vertical position while immersed in a tank of distilled water, as indicated in Figure 5. A transmitting piezoelectric crystal located on one side of a plate generated a pulsed ultrasonic wave. The portion of the ultrasonic energy transmitted through the plate was detected by a second or receiving crystal. The electrical energy generated in the receiving transducer was amplified and fed into a recorder, as seen in Figure 6. By synchronization of the motions of the scanner-recorder, a two-dimensional plot was made of the transmitted signal. Failure to transmit, or scattering of the signal because of voids, porosity, or non-bonds, resulted in a white area on the trace. Discontinuities as small as 1.5 mm (0.063 in.) in diameter can be detected with the apparatus used. Each

plate was scanned at two different attenuations so that core-to-clad and clad-to-clad bonding was investigated.

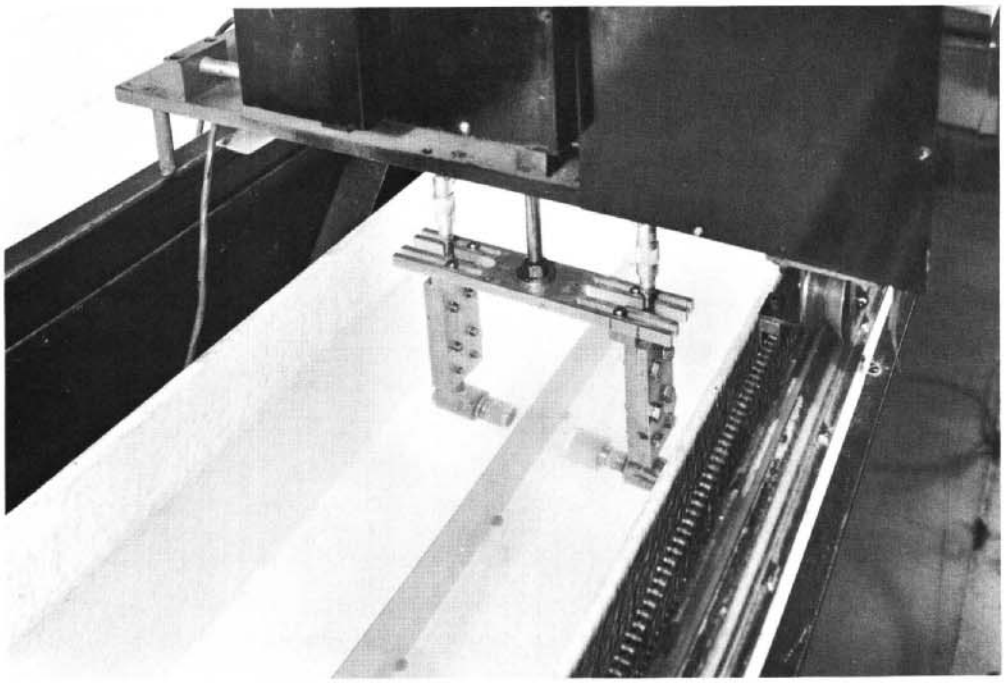

Figure 5. Fuel Plate in Position for Ultrasonic Through-transmission Testing

Figure 6. Ultrasonic Through-transmission Testing Equipment

A zinc sulfide probe in association with a scintillation spectrometer was used to detect radioactive contamination on fuel plate surfaces,(9) as shown in Figure 7. Alpha-energy emission was measured by scanning both sides of each plate with the probe, and the number of counts above background was determined. The minimum contamination detectable with a 99% confidence level was 3-6 μg of fully enriched uranium on any given plate surface.

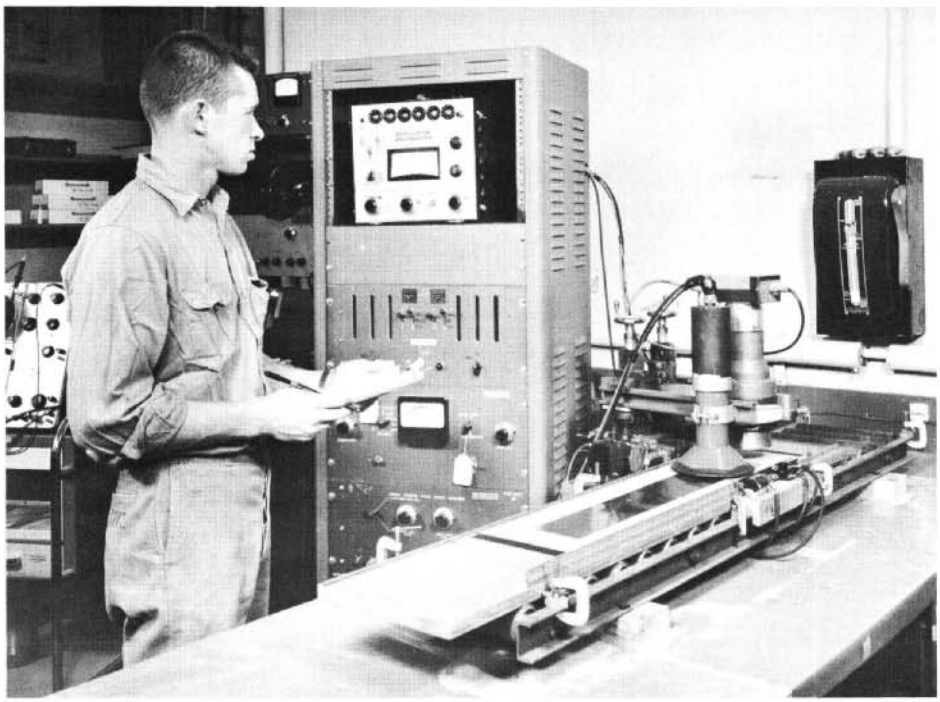

Figure 7. Measurement of Radioactive Surface Contamination of Fuel Plate

The total U^{235} within each individual plate core was determined by counting with a sodium iodide probe in association with a scintillation spectrometer to measure gamma-energy emission. By scanning plates in their entirety and comparing the counts obtained with those obtained from known standards, the U^{235} content of each plate was determined to within $\pm 1.5\%$ of the actual content at the 95% confidence level.

Similar equipment was used to measure the distribution of U^{235} within each plate core. In this case, however, a collimator was used to enable the probe to receive gamma energy from only a 6.45-cm^2 (1-square-inch) area at a time. Four such areas were probed on each plate. The mean amount of gamma emission from the four areas was calculated. The gamma-emission count obtained for each of the areas was then expressed as a percentage deviation from this calculated mean value. The percentage deviations were considered representative of the oxide dispersion within the plate core. A counting error of 1.0% or less was inherent in the equipment.

Gamma energy is infrequently emitted from depleted UO_2. Therefore a reliable determination of U^{235} content or homogeneity within depleted plate cores would necessitate an unduly long counting time. Complete nondestructive testing for these core quantities was, therefore, not performed on depleted plates. The elimination of these tests on depleted plates was justified for two reasons. Wet chemical analysis of depleted evaluation plates would be sufficient to establish plate-core homogeneity and thus qualify the plate-fabrication process. An accurate accounting of depleted UO_2 was not needed to the extent that the long time required for total U^{235} determination was warranted. However, sufficient depleted plates were subjected to these two nondestructive measurements to establish the testing procedures.

With these exceptions, all fuel plates, depleted and enriched, were subjected to a complete nondestructive evaluation.

Destructive Evaluation

The reliability of nondestructive tests which measure bond integrity and core homogeneity can best be substantiated by destructive evaluation. In addition, the dependability of measurements of cladding on face, side, and end, and the characteristics of both UO_2 stringering and particle agglomeration, had to be thoroughly established. Consequently, each of the depleted evaluation plates was sectioned, and samples for metallography, chemical analysis, and corrosion testing were taken, as detailed in Figure 8. Sectioning of enriched plates was done only to confirm the presence of suspected flaws.

Sensitization of austenitic stainless steels involves the intergranular precipitation of chromium carbide and occurs most readily in the approximate temperature range from 425 to 815°C. The resulting reduction in chromium content of the immediate area surrounding each grain therefore promotes susceptibility to corrosive attack. If the carbon content of the steel is not more than 0.03 w/o, carbide formation is inconsequential. Therefore, Type 304-L stainless steel (0.03 w/o carbon maximum) was specified for cladding the BORAX-V superheat fuel.

The acidified copper sulfate (Strauss) test for intergranular corrosion was performed on 6.4 mm x 2.54 cm (0.25 x 1 in.) x plate thickness samples of cladding from both ends of each evaluation plate, and from 10% of the assembly development plates.

End-cladding coupons were taken from both ends of each enriched plate prior to shearing the plates to length. These coupons were shipped to ANL along with the plates, as specified. A random 10% sample of these coupons was also tested for susceptibility to intergranular attack. The procedure followed was as specified in the 1961 ASTM Standards.[10] Each specimen was sensitized at 675°C for 1 hr and subjected to boiling, acidified copper sulfate for 72 hr.

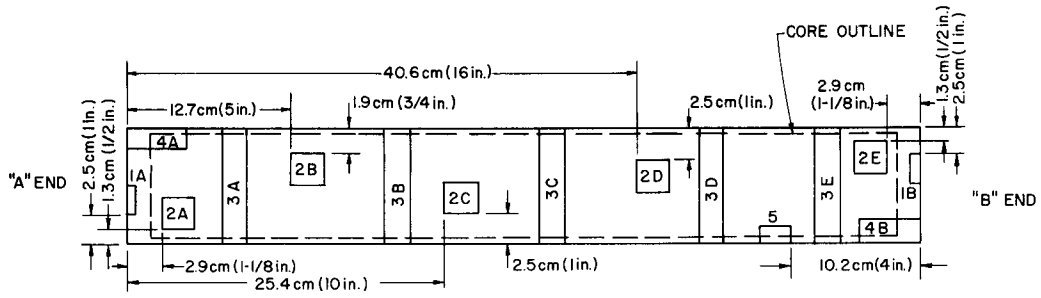

1. "A" end of plate is the end on which identification numbers are stamped.
2. Marking of plate for sectioning was done with identification numbers up or showing. A template placed in proper position over the plate served as a guide for accurate delineation of specimen areas.
3. Sample to destructive test correlation:

   1A, 1B - Sensitization.
   2A, 2B, 2C, 2D, 2E - Homogeneity of core.
   3A, 3B, 3C, 3D, 3E, 4A, 4B - Bond integrity and cladding thickness.
   5 - Oxide fragmentation and stringering.

4. Distances from "A" end of samples numbered 3A, 3B, 3C, 3D, and 3E are 7.6 cm, 20.3 cm, 33.0 cm, and 55.9 cm (3, 8, 13, 18, and 22 in.), respectively.

Figure 8. Fuel-plate Samples Taken for Destructive Evaluation

Samples for chemical analysis of uranium content were taken from five locations on each plate as shown in Figure 8. In order to determine the degree of homogeneity of UO_2 dispersion within the plate core, the stainless steel cladding had to be removed from the samples prior to analysis.(11) Cladding was removed from both sides of each sample simultaneously by clamping the 2.5 x 3.8-cm (1 x 1.50-in.) sample in a holder resembling a hand vise, supporting this holder horizontally in the tool post on the end of a shaper ram, and passing the work back and forth between two HSS tool bits held on the outer faces of opposed work guiding holders. The decladding setup is shown in Figure 9. With a ram speed of 67 strokes/min and a table cross feed of 0.1 mm (0.005 in.) per stroke, each sample was finished in 5 min. The samples as submitted to the Chemistry Division for analysis were 2.5 cm (1 in.) square x 0.27 mm (0.011 in.) thick.

The method used to determine the uranium content of the samples closely resembled that reported by Marley and Kiley.(12) The sample was dissolved in a hydrochloric-nitric acid mixture and fumed with perchloric acid. The constituents of the stainless steel were removed from the perchloric acid solution by mercury-cathode deposition. The uranium was reduced by passing the solution through a lead reductor; the uranium was then titrated with standard ceric sulfate solution containing ferroin indicator. The results obtained with this method are accurate to within ±0.3%.

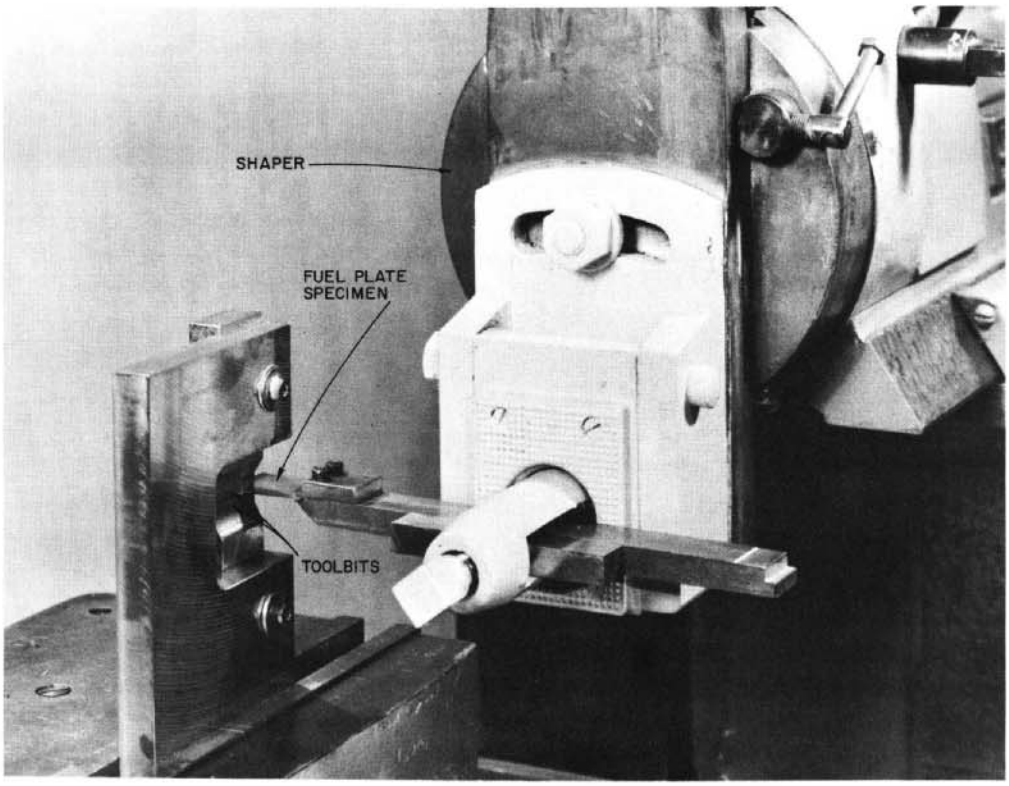

Figure 9. Setup for Decladding Fuel Plate Samples for Chemical Analysis

As shown in Figure 8, five transverse samples and two longitudinal samples were taken from each plate for metallography. The samples were mounted, polished through 1-μ diamond paste, and electrolytically etched with a 5% chromic acid solution. Each specimen was examined at 100X for bond integrity.

Measurements of face cladding and core thickness were taken at 6.4-mm (0.25-in.) intervals along the same samples which were used for determination of bond integrity. Side cladding was measured from the transverse samples and end cladding from the longitudinal samples.

Measurements of maximum stringer lengths, largest particle sizes, and largest particle groups were made from longitudinal samples taken from each plate.

Depleted Plates for Fabrication Evaluation

Correlation and comparison of evaluation data with specifications resulted in the rejection of all 24 of the first plates received for one or more of the following reasons:

1. External plate dimensions were incorrect. The lengths of 10 plates were from 0.05 to 0.10 mm (0.002 to 0.004 in.) over that specified. The widths of 2 plates were 0.03 to 0.05 mm (0.001 to 0.002 in.) too great.

2. Flatness was not within 0.05-mm (0.002-in.) total indicator runout (TIR) per 5.1-cm (2-in.) length. The TIR per 5.1-cm (2-in.) length for 18 plates ranged from 0.08 to 0.28 mm (0.003 to 0.011 in.).

3. Positioning of core relative to the sides was incorrect. As measured from radiographs furnished by the contractor, 12 plates had side cladding ranging from 0.64 to 1.40 mm (0.025 to 0.055 in.) in width and were therefore inadequate. Core widths were, in every case, satisfactory.

Destructive evaluation substantiated the measurements taken from radiographs. A total of 240 side-cladding measurements, ten on each plate, were made. Low or high values of side cladding were found on 12 of the 24 plates. Values from 1.40 to 2.92 mm (0.055 to 0.115 in.) were considered satisfactory.

4. Core length was less than minimum required owing to core ends not being square from side to side. Core lengths were determined by measuring the cladding thickness at plate ends and subtracting these values from plate lengths. Measurements from metallographic samples substantiated the measurements from radiographs. High values of end cladding were found on 6 plates. Of 84 measurements taken, 10 were greater than 2.54 cm (1 in.). Values from 0.64 to 2.54 cm (0.25 to 1 in.) were considered satisfactory.

5. Face-cladding measurements were low and core-thickness measurements were high. There is no nondestructive test for measurement of face cladding and core thicknesses. Consequently, a statistical approach was taken to develop estimates of expected values for those plates which could not be sectioned. It was found that 30-40% of about 3500 face-cladding measurements were not greater than 0.18 mm (>0.007 in.), i.e., were not within specifications. Table III is a compilation of data obtained for face-cladding thicknesses. The measured values of face cladding appeared to be normally distributed about their mean values, as shown in Figure 10. To the extent that they are normally distributed, the standard deviation S is a good measure of the dispersion of sample readings.[13] Approximately 67% of values will fall within ±1.00 S and 95% of values within ±1.96 S of their mean. Based on sample measurements from these initial evaluation plates, it can be expected that approximately 95% of values will fall within 0.18 ± 0.03 mm (0.007 ± 0.001 in.), and 98% will be greater than 0.15 mm (0.006 in.). Oxide particle penetration and localized core thickness variation account for the scattered values between 0.10 mm (0.004 in.) and 0.15 mm

Table III

FACE-CLADDING DATA FROM DEPLETED EVALUATION PLATES

	Top Face					Bottom Face				
Plate Number	Number of Readings	Mean Value*	Range of Values*	Standard Deviation*	Number of Values Not Meeting Specs	Number of Readings	Mean Value*	Range of Values*	Standard Deviation*	Number of Values Not Meeting Specs
FCD 7	73	0.173 (6.8)	0.152-0.203 (6.0-8.0)	0.012 (0.465)	27 (37.0%)	73	0.173 (6.8)	0.152-0.203 (6.0-8.0)	0.011 (0.451)	30 (41.1%)
FCD 8	72	0.173 (6.8)	0.140-0.203 (5.5-8.0)	0.013 (0.512)	33 (45.8%)	72	0.185 (7.3)	0.140-0.216 (5.5-8.5)	0.015 (0.590)	11 (15.3%)
FCD 9	73	0.170 (6.7)	0.152-0.203 (6.0-8.0)	0.013 (0.510)	39 (53.4%)	73	0.180 (7.1)	0.140-0.216 (5.5-8.5)	0.014 (0.570)	20 (27.4%)
FCD 10	73	0.170 (6.7)	0.152-0.203 (6.0-8.0)	0.009 (0.392)	28 (38.4%)	73	0.178 (7.0)	0.152-0.203 (6.0-8.0)	0.009 (0.339)	12 (16.4%)
FCD 13	72	0.170 (6.7)	0.127-0.203 (5.0-8.0)	0.014 (0.541)	36 (50.0%)	72	0.163 (6.4)	0.140-0.191 (5.5-7.5)	0.011 (0.445)	55 (76.0%)
FCD 14	73	0.168 (6.6)	0.140-0.191 (5.5-7.5)	0.013 (0.503)	45 (61.6%)	73	0.173 (6.8)	0.114-0.216 (4.5-8.5)	0.018 (0.706)	35 (47.9%)
FPD 5	73	0.175 (6.9)	0.152-0.203 (6.0-8.0)	0.014 (0.538)	33 (45.2%)	73	0.180 (7.1)	0.140-0.216 (5.5-8.5)	0.015 (0.591)	18 (24.7%)
FPD 7	72	0.180 (7.1)	0.140-0.229 (5.5-9.0)	0.015 (0.592)	24 (33.3%)	72	0.185 (7.3)	0.152-0.216 (6.0-8.5)	0.015 (0.606)	8 (11.1%)
FPD 8	73	0.183 (7.2)	0.152-0.216 (6.0-8.5)	0.011 (0.447)	11 (15.1%)	73	0.185 (7.3)	0.152-0.216 (6.0-8.5)	0.014 (0.550)	10 (13.7%)
FPD 10	73	0.175 (6.9)	0.152-0.203 (6.0-8.0)	0.014 (0.477)	26 (35.6%)	73	0.178 (7.0)	0.140-0.203 (5.5-8.0)	0.013 (0.528)	25 (34.2%)
FPD 12	72	0.183 (7.2)	0.152-0.216 (6.0-8.5)	0.013 (0.525)	10 (13.9%)	72	0.185 (7.3)	0.102-0.216 (4.0-8.5)	0.020 (0.791)	6 (8.3%)
FPD 14	73	0.185 (7.3)	0.152-0.216 (6.0-8.5)	0.012 (0.481)	7 (9.6%)	73	0.191 (7.5)	0.152-0.229 (6.0-9.0)	0.015 (0.595)	7 (9.6%)
HCD 8	73	0.173 (6.8)	0.152-0.216 (6.0-8.5)	0.011 (0.450)	35 (47.9%)	73	0.173 (6.8)	0.152-0.203 (6.0-8.0)	0.012 (0.460)	35 (47.9%)
HCD 10	73	0.175 (6.9)	0.152-0.216 (6.0-8.5)	0.013 (0.520)	33 (45.2%)	73	0.180 (7.1)	0.152-0.203 (6.0-8.0)	0.014 (0.558)	17 (23.3%)
HCD 11	71	0.175 (6.9)	0.152-0.216 (6.0-8.0)	0.013 (0.509)	25 (35.2%)	71	0.183 (7.2)	0.140-0.203 (5.5-8.0)	0.013 (0.501)	11 (15.5%)
HCD 12	73	0.163 (6.4)	0.127-0.216 (5.0-8.0)	0.014 (0.546)	65 (89.0%)	73	0.160 (6.3)	0.127-0.191 (5.0-7.5)	0.015 (0.601)	54 (74.0%)
HCD 13	72	0.178 (7.0)	0.152-0.216 (6.0-8.0)	0.012 (0.486)	16 (22.2%)	72	0.180 (7.1)	0.152-0.203 (6.0-8.0)	0.012 (0.463)	13 (18.1%)
HCD 14	72	0.168 (6.6)	0.152-0.191 (6.0-7.5)	0.011 (0.443)	45 (62.5%)	72	0.175 (6.9)	0.152-0.203 (6.0-8.0)	0.013 (0.497)	24 (33.3%)
HPD 7	73	0.178 (7.0)	0.152-0.203 (6.0-8.0)	0.011 (0.437)	14 (19.2%)	73	0.183 (7.2)	0.152-0.203 (6.0-8.0)	0.013 (0.501)	15 (20.5%)
HPD 8	72	0.175 (6.9)	0.127-0.216 (5.0-8.5)	0.016 (0.618)	23 (31.9%)	72	0.178 (7.0)	0.140-0.203 (5.5-8.0)	0.013 (0.527)	16 (22.2%)
HPD 9	73	0.168 (6.6)	0.127-0.203 (5.0-8.0)	0.014 (0.557)	47 (64.4%)	73	0.168 (6.6)	0.140-0.216 (5.5-8.5)	0.016 (0.621)	46 (63.0%)
HPD 11	73	0.175 (6.9)	0.140-0.203 (5.5-8.0)	0.014 (0.558)	24 (32.9%)	73	0.173 (6.8)	0.140-0.203 (5.5-8.0)	0.014 (0.546)	34 (46.6%)
HPD 12	72	0.165 (6.5)	0.127-0.203 (5.0-8.0)	0.014 (0.569)	49 (68.1%)	72	0.168 (6.6)	0.140-0.203 (5.5-8.0)	0.016 (0.649)	44 (61.1%)
HPD 13	72	0.180 (7.1)	0.152-0.203 (6.0-8.0)	0.011 (0.448)	13 (18.1%)	72	0.178 (7.0)	0.127-0.203 (5.0-8.0)	0.014 (0.546)	15 (20.8%)
Totals and Averages	1741	0.175 (6.9)	0.127-0.229 (5.0-9.0)	0.013 (0.505)	698 (40.1%)	1741	0.178 (7.0)	0.102-0.229 (4.0-9.0)	0.013 (0.551)	571 (32.8%)
Grand Totals and Averages						3482		0.102-0.229 (4.0-9.0)	0.013 (0.528)	1269 or 36.4% too low

*Values given in mm (mils).

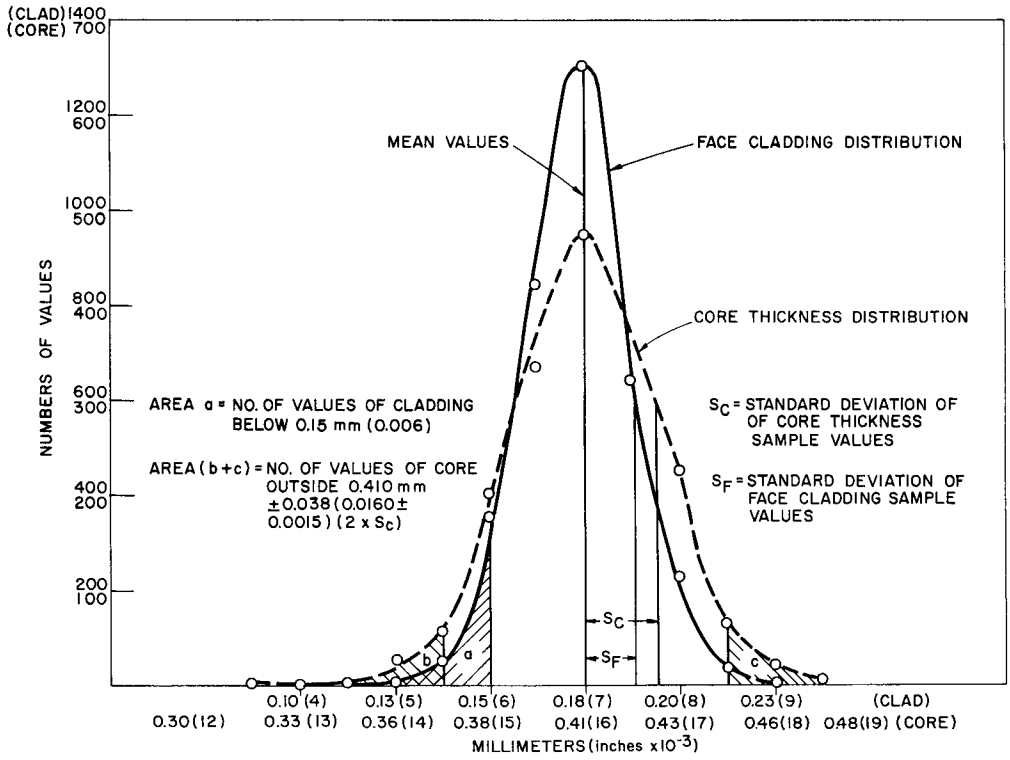

Figure 10. Distribution of Face Cladding and Core Thickness Sample Values from Depleted Evaluation Plates

(0.006 in.). In Figure 11 examples are shown of oxide particles which have penetrated and reduced the effective cladding thickness to 0.10 mm (0.004 in.) and 0.13 mm (0.005 in.) at two locations. In a similar manner, measurements of core thickness as given in Table IV are distributed about their mean (see Figure 10). Approximately 95% of values can be expected to fall within 0.41 ± 0.04 mm (0.016 ± 0.0015 in.) with local thickness variations accounting for scattered values as low as 0.32 mm (0.0125 in.) and as high as 0.47 mm (0.0185 in.).

6. Distribution of uranium in the core blends was inhomogeneous. As had been suspected because of the streaked appearance of the plate cores as seen on their radiographs, homogeneity was unsatisfactory. For each plate the wet chemistry analysis for uranium on each of 5 samples was expressed on a weight percent of sample basis. In only three cases did all the sample values for a given plate core fall within the specified ±3% of the mean of the five sample values. Individual values within a group of 5 deviated as much as 10% from the mean of the 5 sample values. The only discernible trend was an inverse relationship between precision of group values and UO_2 content of plate cores. The higher the UO_2 content of the plate cores, the more nearly homogeneous were the core blends. This relationship becomes obvious when the limiting cases are considered. A solidly packed UO_2 core (100% UO_2, 0% SS) is inherently homogeneous. At the other extreme, the homogeneity of a core containing one sieve-size, UO_2 particle depends entirely on the position of that particle within the core.

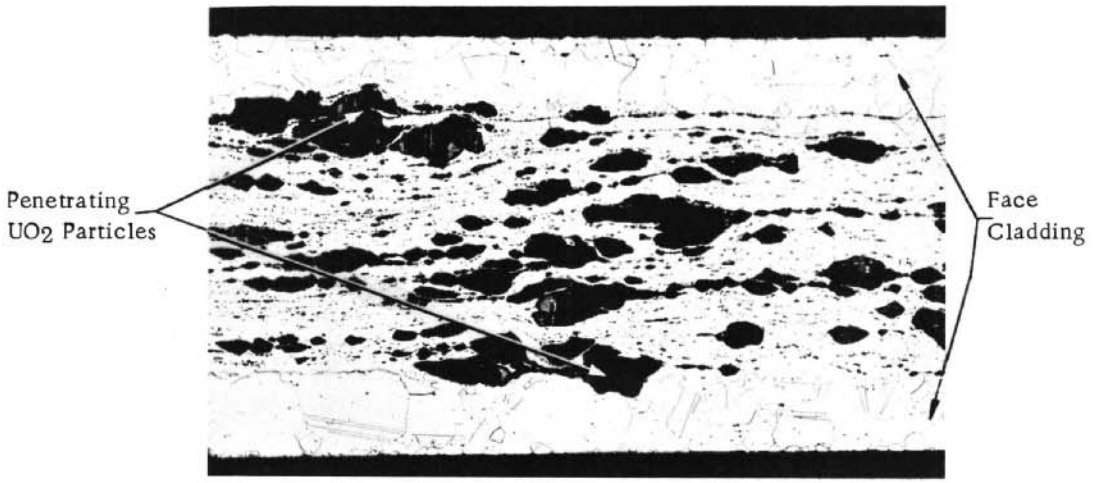

Figure 11. Oxide Particle Penetration into Face Cladding - Depleted Evaluation Plates

Table IV

CORE-THICKNESS DATA FOR DEPLETED EVALUATION PLATES

Plate Number	Number of Readings	Mean Value*	Range of Values*	Standard Deviation*	Number of Values Not Meeting Specs	Plate Number	Number of Readings	Mean Value*	Range of Values*	Standard Deviation*	Number of Values Not Meeting Specs
FCD 7	73	0.417 (16.4)	0.381-0.457 (15.0-18.0)	0.016 (0.637)	71 (97.3%)	HCD 8	73	0.401 (15.8)	0.356-0.445 (14.0-17.5)	0.019 (0.730)	57 (78.1%)
FCD 8	72	0.409 (16.1)	0.356-0.457 (14.0-18.0)	0.023 (0.915)	59 (81.9%)	HCD 10	73	0.401 (15.8)	0.356-0.445 (14.0-17.5)	0.019 (0.738)	57 (78.1%)
FCD 9	73	0.401 (15.8)	0.368-0.432 (14.5-17.0)	0.017 (0.673)	59 (80.8%)	HCD 11	71	0.414 (16.3)	0.381-0.470 (15.0-18.5)	0.018 (0.698)	66 (93.0%)
FCD 10	73	0.409 (16.1)	0.356-0.445 (14.0-17.5)	0.017 (0.673)	64 (87.7%)	HCD 12	73	0.419 (16.5)	0.381-0.470 (15.0-18.5)	0.017 (0.687)	71 (97.3%)
FCD 13	72	0.424 (16.7)	0.381-0.457 (15.0-18.0)	0.015 (0.574)	71 (98.6%)	HCD 13	72	0.401 (15.8)	0.356-0.457 (14.0-18.0)	0.019 (0.732)	55 (76.4%)
FCD 14	73	0.414 (16.3)	0.368-0.457 (14.5-18.0)	0.021 (0.840)	65 (89.0%)	HCD 14	72	0.406 (16.0)	0.356-0.457 (14.0-18.0)	0.019 (0.763)	65 (90.3%)
FPD 5	73	0.406 (16.0)	0.356-0.457 (14.0-18.0)	0.018 (0.725)	64 (87.7%)	HPD 7	73	0.396 (15.6)	0.356-0.445 (14.0-17.5)	0.020 (0.779)	51 (69.9%)
FPD 7	72	0.399 (15.7)	0.318-0.457 (12.5-18.0)	0.028 (1.084)	53 (73.6%)	HPD 8	72	0.401 (15.8)	0.343-0.445 (13.5-17.5)	0.022 (0.885)	51 (70.8%)
FPD 8	73	0.406 (16.0)	0.356-0.470 (14.0-18.5)	0.021 (0.816)	63 (86.3%)	HPD 9	73	0.411 (16.2)	0.368/0.470 (14.5-18.5)	0.022 (0.850)	65 (89.0%)
FPD 10	73	0.401 (15.8)	0.368-0.432 (14.5-17.0)	0.015 (0.594)	63 (86.3%)	HPD 11	73	0.401 (15.8)	0.368-0.432 (14.5-17.0)	0.018 (0.694)	57 (78.1%)
FPD 12	72	0.399 (15.7)	0.356-0.457 (14.0-18.0)	0.016 (0.627)	60 (83.3%)	HPD 12	72	0.411 (16.2)	0.368-0.457 (14.5-18.0)	0.021 (0.810)	60 (83.3%)
FPD 14	73	0.399 (15.7)	0.318-0.445 (12.5-17.5)	0.025 (0.982)	51 (69.9%)	HPD 13	72	0.399 (15.7)	0.330-0.445 (13.0-17.5)	0.021 (0.820)	54 (75.0%)
Totals and Averages							1741	0.406 (16.0)	0.318-0.470 (12.5-18.5)	0.019 (0.764)	1450 or 83.2% too high

*Values given in mm (mils).

The mean of sample values does not necessarily equal the weight percent uranium in a sample taken from a truly homogeneous core. Therefore, the weights of UO_2 and stainless steel powders used by the contractor in blending core materials were used to calculate the weight

percent uranium in each type loading. The actual sample values for a given plate type differed from the calculated value by as much as 20%.

7. UO_2 stringering and particle grouping were excessive. They are both causes of inhomogeneity. As suspected from the results of chemical analysis and confirmed by metallographic examination, stringering and particle grouping are more prominent in plates containing larger amounts of UO_2.

Since a larger total number of particles are present in plates containing more UO_2 in their cores, the probability is higher that groupings or stringers will be formed. Nonsegmented strings of UO_2 particles longer than 0.25 mm (0.01 in.) were found in eight of the first 24 plates examined. A typical stringer, 0.56 mm (0.022 in.) long, is shown in Figure 12.

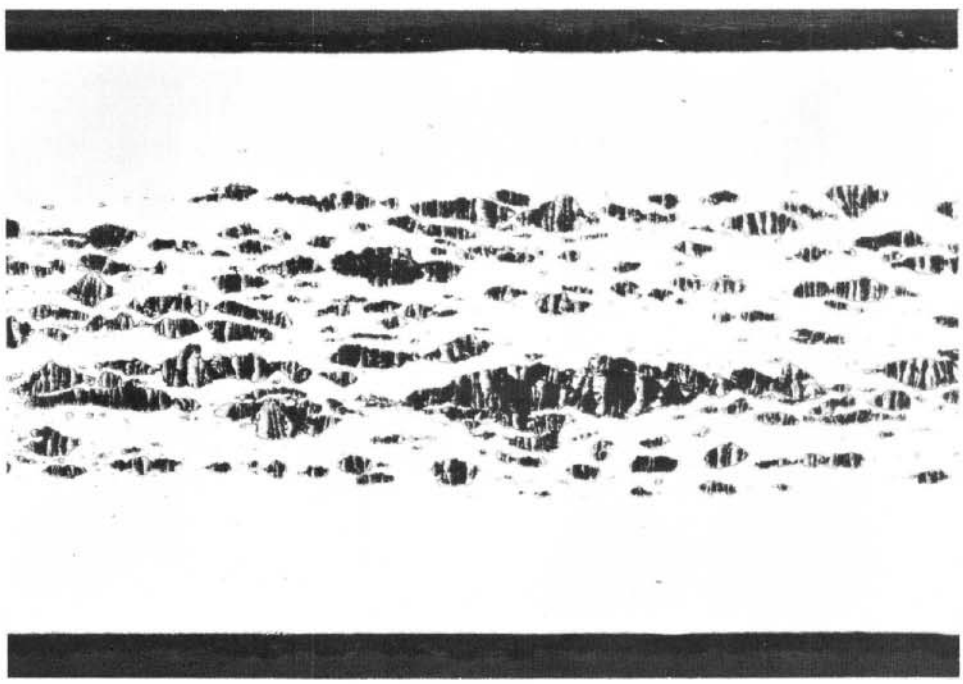

Micro 32208 100X

Figure 12. UO_2 Stringering from a Depleted Evaluation Plate

8. The carbon content of the cladding material was greater than 0.03 w/o. Of the samples subjected to the standard Strauss test, only one, from plate FPD 8, exhibited extensive grain-boundary cracking upon being bent 180° around a mandrel of 3.2-mm (0.125-in.) diameter. A second sample from the same end of this plate did not exhibit the extensive cracking upon bending. Metallographic examination of a piece taken from the cracked specimen showed a continuous network of carbides at the grain boundaries, as seen in Figure 13. Grain-boundary carbides were found to various extents in samples taken from other tested and bent cladding

specimens. However, the carbide networks were not as heavy nor as a continuous as in the former case. Analyses for carbon content were performed on end-cladding samples from plate FPD 8 and from 3 other depleted plates chosen at random. A 0.04 w/o carbon content was reported for the cladding from plate FPD 8, whereas the carbon content of the samples from the other three plates was reported to be 0.03 w/o.

Figure 13. Grain-boundary Carbides in Strauss-tested End Cladding of Depleted Evaluation Plate (FPD 8)

The susceptibility to carbide precipitation which was evidenced in end cladding from only one depleted evaluation plate was an anomaly not likely to be encountered in the enriched plates. It appears that carbon contamination was locally introduced from an external source, causing an isolated zone of cladding to be higher in carbon content than is ordinary 304-L SS. Since the bulk analysis performed on the end cladding from this plate indicated a carbon content of 0.04 w/o, and since the grain-boundary carbides near the surface were heavy and continuous, it is most likely that the outer layer of cladding was even higher in carbon content than the bulk analysis indicated, whereas the unexposed and uncontaminated material was, in reality, 304-L SS. Close control during enriched-plate production should eliminate such contamination.

The most noteworthy of the areas in which no difficulty was encountered is that of achieving an integral clad-to-clad or core-to-clad bond. No evidence of non-bonds was found during ultrasonic through-transmission testing or during metallographic examination.

The incorrect dimensions found for plate, core, and cladding did not cause much concern, for minor adjustments in processing procedures should adequately correct these discrepancies.

The unsatisfactory degree of plate-core homogeneity and the poor control of oxide stringering were not only the most undesirable of the known departures from specifications, but were expected to be the most difficult to correct. In order to improve the accuracy of reported plate oxide contents, the contractor agreed to weigh and blend each plate core individually rather than use the batch weighing and blending techniques originally employed. This process revision plus improved blending techniques were expected to improve the precision of the values of uranium content obtained from unit-core volumes for any given plate. Since stringering was most prominent in type FPD plates and homogeneity is hardest to achieve in type HCD plates, it was agreed that AI would next fabricate six each of these two plate types by the revised procedures. The plates were delivered to ANL and evaluated as previously outlined. Some departures from specifications still were found as listed below:

1. pits and impressions on plate surfaces;
2. slightly excessive plate lengths;
3. wide cores and deficient side cladding on type FPD plates;
4. high measurements of core thickness due to distribution around a mean value of 0.38 mm (0.015 in.) rather than of 0.36 mm (0.014 in.);
5. inhomogeneous distribution of uranium in the core blends;
6. excessive stringer lengths and large particle groups in type FPD plates;
7. excessive oxide particle sizes.

Although this list of discrepancies appears to be sufficient cause for rejection of the plates, they were, in fact, accepted. Items 1 through 4 pertain to defects which are quite easily remedied by applying minor adjustments and controls to production variables. Homogeneity (Item 5) was markedly improved over that achieved in the first plates fabricated, although still not within the ±2 w/o of the amount present as specified. Stringering and particle grouping (Item 6) was not nearly as excessive as previously found, but lengths of nonsegmented UO_2 particles greater than 0.38 mm (0.015 in.) were still found in type FPD plates. The fabricator agreed to screen and remove all UO_2 particles outside the size range of 37-88 μ. Elimination of large particles (Item 7) was expected to improve both the homogeneity and the stringering and particle-grouping characteristics of plates subsequently fabricated. Supplemental Agreement No. 1 (see Appendix A) to Subcontract 31-109-38-1252 was then drawn up revising specifications in two areas:

1. Maximum UO_2 stringer length allowable was increased from 0.25 mm (0.01 in.) to 0.5 mm (0.02 in.).

2. Allowable variation from true homogeneity of uranium content in the plate cores was increased from ±2 w/o to ±5 w/o of the amount present.

No further difficulty was anticipated in fabricating fuel plates to meet the specifications as revised.

The plates accepted (types HCD and FPD) represented only half of the specified number of depleted evaluation plates. The fabricator was still required to deliver six each of the type FCD and HPD plates, representing the other half of the total specified. The plates were fabricated, delivered, and inspected by the standard procedures. These plates were accepted. Although some isolated cladding measurements did not meet the specifications, the vast majority of measurements were within the allowable tolerances.

Depleted Plates for Assembly Development

The 160 depleted plates which were used for development of assembly operations were evaluated by means of the same nondestructive tests used for evaluation of the first depleted plates delivered to ANL.

During the nondestructive testing for bond integrity, the plates were immersed in a tank of distilled water for about $\frac{1}{2}$ hr. Rust-colored stains appeared on the surfaces of some of these depleted plates during the testing period. Metallographic examination of these stained areas proved the existence of imbedded particles which, judging from the color of the corrosion product, were most likely ferritic in nature. The source of the particles was traced to a chilled iron-grit blast used by the contractor to clean picture frame and cover-plate components before assembly of rolling compacts. The contractor then began acid pickling the grit-blasted components before assembly of compacts for rolling in an effort to remove the imbedded iron particles. The plates were satisfactory in every other aspect, and they were accepted with the understanding that enriched fuel plates exhibiting similar surface defects would not be acceptable. All of the plates inspected were accepted.

Enriched Plates

Of the original 840 enriched plates fabricated, 16 were destructively evaluated by the fabricator. These plates were selected for evaluation by ANL during the fabrication period as representative samples of 2% of each of the four plate types. All plates were accepted by the Laboratory.

The remaining 824 plates were nondestructively tested as outlined in Figure 1. A total of 28 plates were rejected for reasons as given in Table V. Of the 28 plates rejected, 3 did not pass the ultrasonic through-transmission test. The defect in one plate was indicated as measuring 0.32 cm x 0.95 cm (0.125 in. x 0.375 in.) on a recording of transmitted energy. Upon metallographic examination, the defect was found to be a lamination within the plate core, as seen in Figure 14. In another instance, the bond test indicated a 1.27 x 0.63-cm (0.500 x 0.250-in.) flaw which was found to be a dense core inclusion, as seen in Figure 15. The third flaw, measuring 0.16 cm x 0.48 cm (0.062 in. x 0.187 in.), did not have to be destructively verified, since a barely perceptible surface blister was evidence that a core-to-clad non-bond was present at that location.

Table V

SUMMARY OF ENRICHED FUEL PLATES REJECTED

Plate Type	Number Inspected	Number Rejected	Reasons for Rejection
HCE	192	2	1 - Core lamination 0.32 cm (0.125 in.) x 0.95 cm (0.375 in.) as detected by ultrasonic through-transmission test.
			1 - Many small corrosion stains on the plate surfaces after immersion in ambient distilled water.
FCE	195	5	1 - Inadequate cladding along one side of the plate, as measured from radiograph.
			1 - Low total U^{235} content in the core as measured by gamma-energy emission.
			3 - Plate width and squareness (TIR) not within tolerance.
HPE	233	3	1 - Non-bond between core and cladding measuring 0.16 cm (0.062 in.) x 0.48 cm (0.187 in.) as detected by ultrasonic through-transmission test.
			2 - Inadequate cladding along one side of each plate, as measured from radiograph.
FPE	248	18	1 - Dense core inclusion, 1.3 cm (0.5 in.) x 0.6 cm (0.25 in.), as detected by ultrasonic through-transmission test.
			3 - Inadequate cladding along one side of each plate, as measured from radiograph.
			14 - Plate thicknesses less than minimum specified.

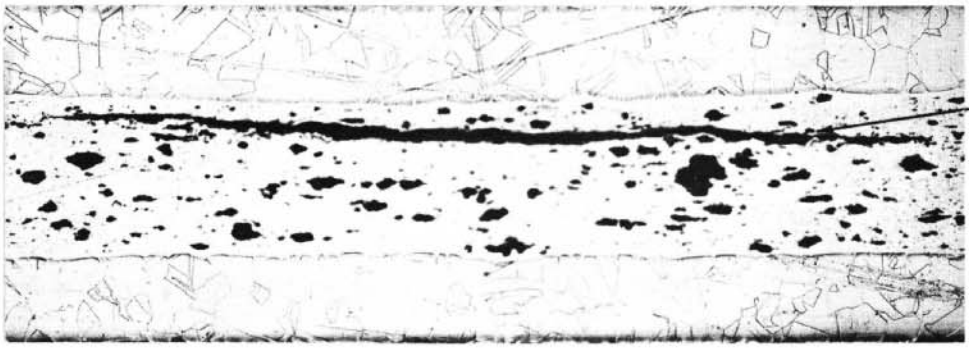

Micro 33460 50X

14a. Fuel-plate core lamination

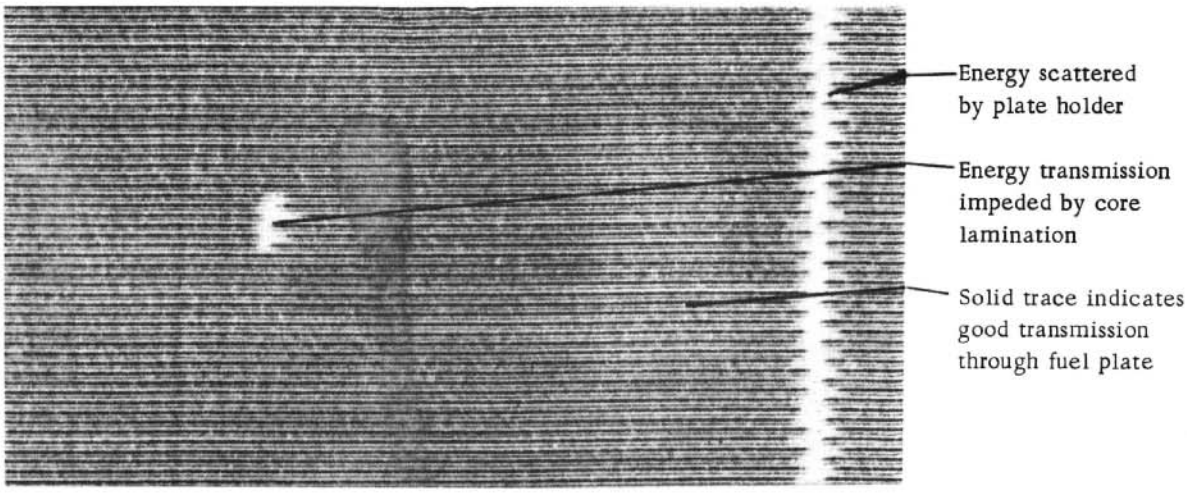

14b. Recording of energy transmitted through section of fuel plate containing lamination

Figure 14. Core Lamination Detected by Ultrasonic Through-transmission Testing

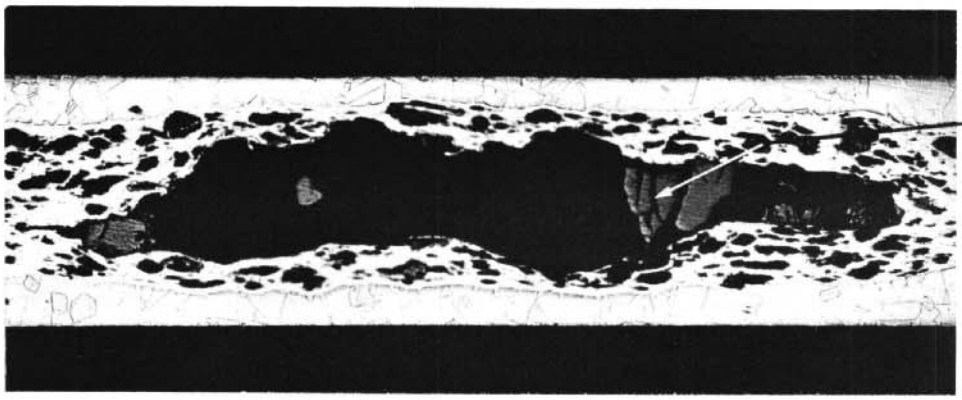

Micro 35119 50X

15a. Fuel-plate core inclusion

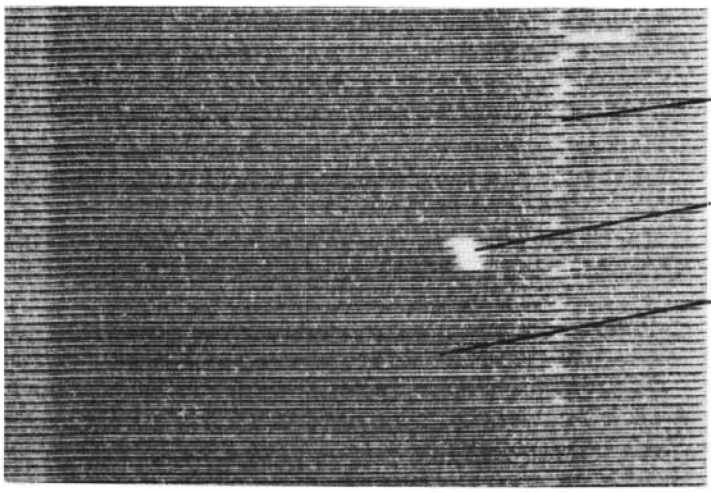

15b. Recording of energy transmitted through section of fuel plate containing inclusion

Figure 15. Core Inclusion Detected by Ultrasonic Through-transmission Testing

One of the 14 plates, rejected because the thickness was less than that specified, was sectioned for metallography. Face cladding was found to be thinner than the 0.18-mm (0.007-in.) minimum required. Owing to the nominal thinness of the face cladding on these fuel plates, any reduction in this dimension could not be tolerated.

The 6 plates having inadequate side cladding, 3 plates having improper widths and squareness, and 1 plate exhibiting surface corrosion stains could obviously be rejected without destructive verification. Since the contractor agreed with the nondestructive results by which one plate was rejected as having a low content of U^{235} in the core, there was no need for wet chemical analysis. Replacements for these rejected plates were subsequently received, inspected, and accepted.

EVALUATION SUMMARY

The nondestructive test data coupled with the destructive examination of the depleted evaluation plates and selected enriched plates, enables a high degree of confidence to be placed in the following beliefs as to the quality of the fuel in BORAX-V Superheat Fuel Elements:

1. There is a good dispersion of UO_2 particles within the plate cores. Typical transverse and longitudinal structures of cores are seen in Figure 16. No UO_2 stringers longer than 0.5 mm (0.02 in.) were found in either the second set of depleted evaluation plates or those enriched plates which were destructively examined. Screening of UO_2 particles was done to eliminate particles outside the size range of 37 to 88 μ. A minimum of particle grouping was found in those plates examined subsequent to the first set of depleted evaluation plates.

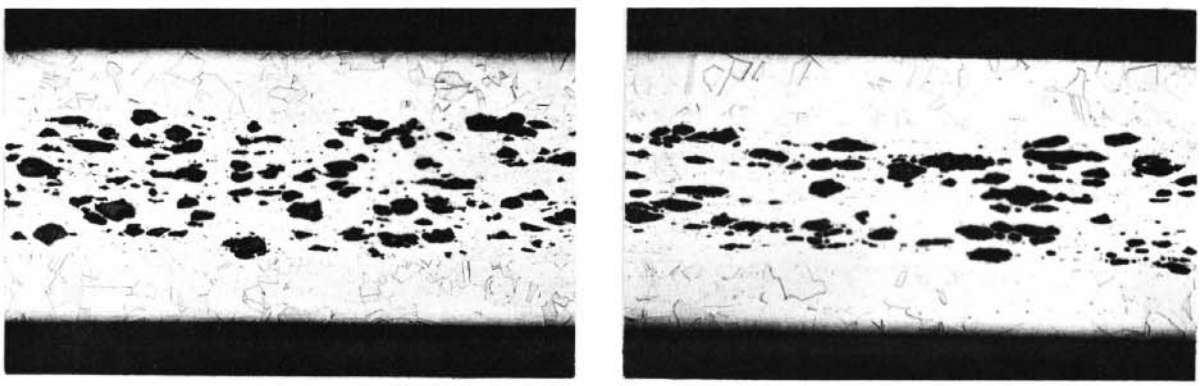

Micro 33232 50X
Transverse section through fuel plate

Micro 33233 50X
Longitudinal section through fuel plate

Figure 16. Typical Core Structure in BORAX-V Superheat Fuel Plates

2. Each plate has integral core-to-clad and clad-to-clad bonding, as shown in Figure 17. The capabilities of the ultrasonic through-transmission testing equipment are such that nonbonds 1.6 mm (0.06 in.) in diameter or larger could be detected. It is common for externally visible blisters to appear on the fuel plate surfaces at locations of nonbonds. Therefore a thorough visual surface inspection was used to supplement the ultrasonic test.

3. The core homogeneity within each plate is such that the amount of uranium in a 6.5-cm^2 (1-sq in.) plate-core sample will not vary by more than ±5% from the average w/o of contained uranium for the entire plate core. Some values obtained during nondestructive testing of the enriched plates were outside this range, although fluctuations in core and/or cladding thicknesses may have been the cause of these extreme values [i.e., the scintillation spectrometer cannot distinguish

between (1) gamma-count variations caused by departures from a true uniform dispersion of uranium within the plate core, and (2) gamma-count variations caused by changing thicknesses of a core which actually contains a true uniform dispersion of uranium].

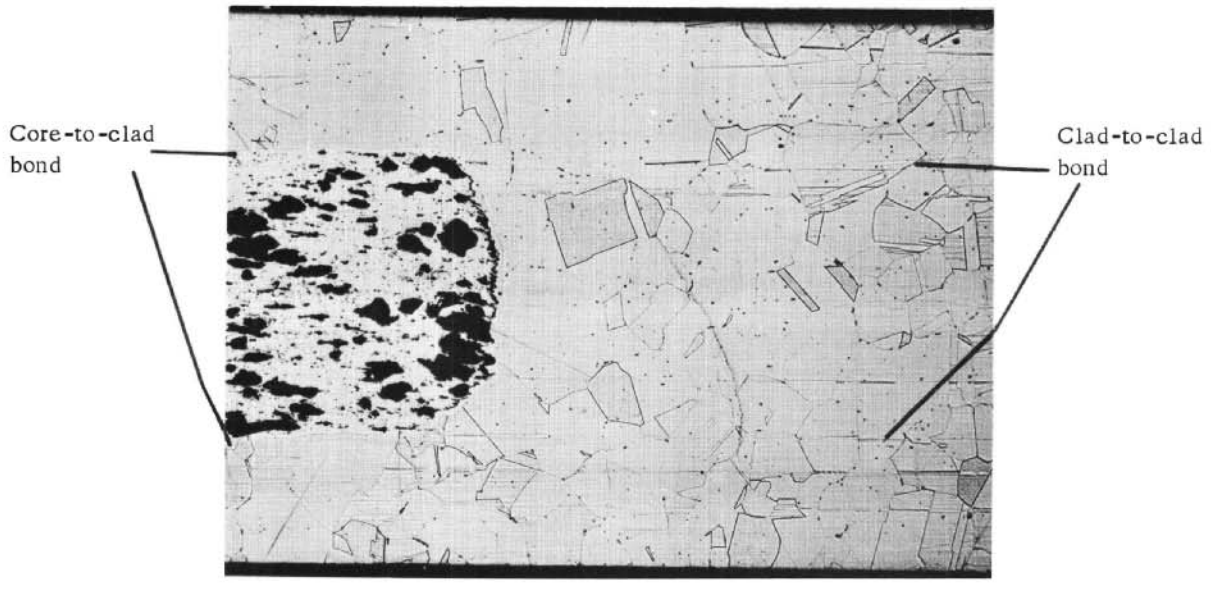

Micro 36910 100X

17a. Bond characteristics at side of fuel plate

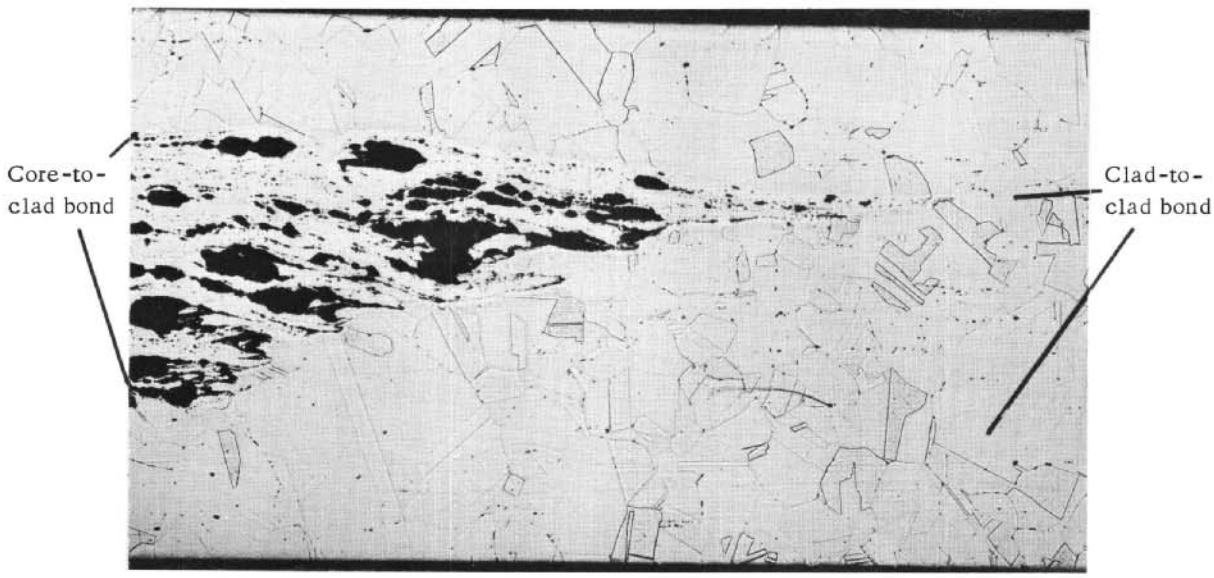

Micro 36909 100X

17b. Bond characteristics at end of fuel plate

Figure 17. Bond Characteristics in BORAX-V Superheat Fuel Plates

From the results of chemical analyses of core samples from the evaluation plates, the 2 sigma limits for w/o uranium in the chemistry

samples were calculated, as shown in Appendix B. These limits bracket the range within which 95% of all sample values fall. Since these calculations were based on a large number of measurements and all enriched plates were fabricated by use of procedures identical with those used in processing the plates from which the measurements were taken, it is expected that actual 2 sigma limits are closely approximated by those calculated, as shown in Table VI. The machining operation to remove cladding from chemistry samples may have introduced some error into the final results, because some UO_2 particles were undoubtedly pulled out of the exposed core surfaces. It is equally likely that the number of particles removed varied from sample to sample.

Table VI

PROBABLE CORE HOMOGENEITY BASED ON STATISTICAL ANALYSIS - ENRICHED FUEL PLATES

Type of Fuel Plate	w/o Contained Uranium (Avg)	2 Sigma (95% Range - w/o U)	Homogeneity (% Deviation from Avg)
Half Central	10.16	9.58-10.74	±5.70
Full Central	19.01	18.44-19.61	±3.15
Half Peripheral	16.43	15.95-16.91	±2.92
Full Peripheral	27.99	26.87-29.11	±4.00

4. The average core and cladding thicknesses, as given in Tables VII and VIII, approach nominal specifications. The 2 sigma values were calculated from data gathered during destructive evaluation of the second set of depleted evaluation plates. Although the average face cladding was somewhat thinner than the 0.20 mm (0.008 in.) nominal, 95% of the integral face cladding area should be within the 0.15-0.23 mm (0.006-0.009 in.) range of thicknesses. Local UO_2 particle penetration

Table VII

PROBABLE FACE-CLADDING THICKNESS BASED ON STATISTICAL ANALYSIS - ENRICHED FUEL PLATES

Type of Fuel Plate	Average Face Cladding, cm (in.)	2 Sigma [95% Range, cm (in.)]
Half Central	0.0193 (0.0076)	0.0152-0.0234 (0.0060-0.0092)
Full Central	0.0193 (0.0076)	0.0163-0.0223 (0.0064-0.0088)
Half Peripheral	0.0196 (0.0077)	0.0168-0.0223 (0.0066-0.0088)
Full Peripheral	0.0196 (0.0077)	0.0163-0.0229 (0.0064-0.0090)

Table VIII

PROBABLE CORE THICKNESS BASED ON STATISTICAL ANALYSIS - ENRICHED FUEL PLATES

Type of Fuel Plate	Average Core Thickness, cm (in.)	2 Sigma [95% Range, cm (in.)]
Half Central	0.0376 (0.0148)	0.0333-0.0419 (0.0131-0.0165)
Full Central	0.0368 (0.0145)	0.0335-0.0401 (0.0132-0.0158)
Half Peripheral	0.0371 (0.0146)	0.0335-0.0406 (0.0132-0.0160)
Full Peripheral	0.0381 (0.0150)	0.0340-0.0422 (0.0134-0.0166)

into the cladding causes a minimal amount of point thinning to 0.10 mm (0.004 in.). Average core thickness is slightly greater than the nominal 0.36 mm (0.014 in.), with 95% of integral core thickness area within the 0.33-0.43 mm (0.013-0.017 in.) range.

In every plate destructively examined, there were some measured values of face cladding and core thicknesses which were not within specifications. However, the average of all measured values were very nearly nominal, and the vast majority of values were actually within specified limits. The consistency of the dispersions of these measured values about their means leads to the conclusion that the dispersion characteristics are an inherent result of the plate-fabrication process. The adjustment of the dispersions so that all values fell within the specified limits would have required a time-consuming development program which could not be justified on the basis that minor dimensional corrections would have been achieved. The scattered dimensional deviations were deemed acceptable.

5. The total U^{235} content for each plate type, as shown in Table IX, is within specifications. The 2 sigma values were calculated from data obtained by gamma-ray scintillation spectrometry analysis. Although no wet chemical analysis was done to verify the nondestructive test results, a correlation was made among the ANL analyses, the production data reported by AI, and the U^{235} loadings required by contract specification, and is given in Table X. For each plate type, the gamma-ray analysis agreed closely with the production data reported by AI. The range bracketed when the calculated 2 sigma limits were applied to the mean values of U^{235} per plate calculated from ANL analysis was well within the range of values specified. In fact, the 3 sigma limits, within which greater than 99% of all sample values fall,

were also within the specified limits. The probability is very small that ANL analysis and AI production data are both grossly in error and yet agree so closely.

Table IX

PROBABLE TOTAL U^{235} CONTENT BASED ON STATISTICAL ANALYSIS - ENRICHED FUEL PLATES

Plate Type	Average U^{235} per Plate (Nondestructive Analysis)(g)	Standard Deviation of Analytical Values (g U^{235})	2 Sigma Range (g U^{235})
HCE	15.041	0.061	14.919-15.163
FCE	27.882	0.128	27.626-28.138
HPE	23.603	0.106	23.391-23.815
FPE	44.300	0.116	44.068-44.532

Table X

CORRELATION OF TOTAL U^{235} CONTENT ANALYSIS WITH PRODUCTION DATA AND LIMITS SPECIFIED - ENRICHED FUEL PLATES

Type of Loading	Number of Plates	Total U^{235} per Loading (Reported by AI from Production Data [g])	Total U^{235} per Loading (Determined by Scintillation Spectrometry Analysis [g])	Average U^{235} per Plate Required by Contract Specification (g)	Average U^{235} per Plate (Calculated from AI Production Data [g])	Average U^{235} per Plate (Calculated from Scintillation Spectrometry Analysis [g])	Deviation of Scintillation Spectrometry Analysis from AI Production Data (Percent)
HCE	186	2,783.57	2,797.66	14.98 ± 0.32	14.965	15.041	+ 0.51
FCE	186	5,240.24	5,185.99	27.92 ± 0.60	28.173	27.882	- 1.04
HPE	226	5,341.89	5,334.21	23.66 ± 0.51	23.637	23.603	- 0.14
FPE	226	9,974.47	10,012.73	44.21 ± 0.95	44.135	44.30	+ 0.38
Total	824	23,340.17	23,330.59				

6. The plate cladding is insensitive to carbide precipitation and to resultant intergranular corrosion. This conclusion is drawn from inability to produce accelerated grain-boundary corrosion by Strauss tests on end-cladding samples from a randomly selected sample of 10% of all depleted development and enriched fuel plates.

In addition to the plate characteristics, which were established by statistical analysis, overall plate dimensions, flatness, squareness, and radioactive surface contamination were directly measured for each plate and were found to be acceptable. End cladding, side cladding, and core dimensions, as measured from plate radiographs, were within specifications.

ASSEMBLY OF FUEL ELEMENTS

The development of assembly procedures and the assembly of the fuel were done by Central Shops Department of Technical Services Division at ANL, with technical consultation and other assistance from the Metallurgy Division. Preliminary development work was required to determine the most appropriate type of spacers between subassembly fuel plates, to investigate various methods of fastening fuel plates into subassembly positions, and to establish brazing and welding parameters.

For the central superheat fuel loading, 13 standard and 3 instrumented elements were fabricated. For the peripheral superheat fuel loading, 17 standard and 2 instrumented elements were fabricated.

Subassembly Development

Two features of subassembly design that were developed are the type of spacing between the fuel plates and the method of fastening subassembly components into a single unit. The fuel plates were to be spaced at the longitudinal edges by comb-type side strips of Type 304 stainless steel. The high width-to-thickness ratio (>100:1) of the fuel plates made it mandatory that additional support in the form of spacers between plates be provided to insure sufficient rigidity and dimensional stability of the coolant channel. Two methods of spacing were proposed. The first consisted of using 0.32-cm (0.125-in.) diameter, 0.16-cm (0.0625-in.) high buttons or studs located in two parallel rows on 2.86-cm (1.125-in.) centers. Tentative methods for attaching these studs to the fuel plates were mechanical fastening, resistance spot welding, and brazing. Mechanical fastening as proposed would necessitate drilling through the plates and then inserting a bolt or stud with washers between the plates to act as spacers. The entire bolted assembly could then be brazed to seal off areas of exposed core material which might otherwise contact the coolant stream. This procedure was considered too complicated and unreliable to justify extensive development.

Studs fastened by resistance spot welding would be acceptable if the isolated heat generated in the core or cladding was not detrimental. Figure 18 shows a transverse section through a clad plate which was heated by resistance spot welding. Because of the greater resistance offered by the oxide core material, the center of the plate became hotter than the surface in contact with the stud, with the result that uranium oxide was dispersed away from the heated area and in some instances was expelled almost to the plate surface. The possibility of oxide contamination of the plate surface from this method of attaching studs did not justify any further investigation.

The feasibility of vacuum furnace brazing the spacer studs to fuel plates was established with Nicrobraze 50* (nominal composition 13 w/o Cr,

*Manufactured by Wall-Colmonoy Corp., Detroit, Michigan.

10w/o P, 0.15 w/o C, balance Ni) brazing alloy. Joints brazed with Nicrobraze 50 were inherently brittle. Brazed joints would crack during handling and removal of the fixtures used to locate and hold the studs in position between the fuel plates while brazing. It was also difficult to maintain proper alignment of the studs between the fuel plates. Consequently, this method of spacing the plates was discontinued.

Micro 27650 50X

Figure 18. Effect of Resistance Spot Welding on Fuel Plate

The second method of spacing proposed, and that which was used in fabricating the fuel subassemblies, consisted of fastening two 0.16-cm (0.0625-in.) x 61.6-cm (24.25-in.) long, square stainless steel wires, on 2.86-cm (1.125-in.) centers. A condenser-discharge type of spot weld was used to locate the wires on the fuel plates for brazing. Each spacer wire was coined such that the two wire sides to be bonded to fuel plates had 0.16-cm (0.0625-in.) long land areas raised 0.004 cm (0.0015 in.) from the wire proper. These land areas, spaced apart on 7.78-cm (3.0625-in.) centers, performed two functions: 1) During tack welding of the spacer wires to the plates, the lands were the only areas in contact with the plate surface. Welding current was therefore effectively concentrated at the desired location. 2) The 0.038-mm (0.0015-in.) spacing between the wire body and the fuel plate was more conducive to proper flowing of brazing alloy and thorough bonding at the wire-to-plate interface.

Since Nicrobraze 50 resulted in an inherently brittle joint, any alloy containing phosphorus (the constituent contributing greatly to brittleness) fell into immediate disfavor. Alloys containing silicon rather than phosphorus generally produce joints with relatively high ductility, and attention was thus shifted to this general category. Also, experience at Oak Ridge National Laboratory[14] had shown that when Coast Metals 60* (nominally 20 w/o chromium, 10 w/o silicon, 3 w/o iron, balance nickel) was used to braze assemblies of Enrico Fermi plates,[15] a consistently clean, bright joint was attained. It was then established that, if the stainless steel components of a fuel subassembly are held at the brazing temperature (1160°C) for up to 2 hr, sufficient silicon diffuses away from the

*Manufactured by Coast Metals, Inc., Little Ferry, New Jersey.

interface areas to produce strong, ductile metallurgical bonding. Extensive metallographic examination of fuel-subassembly brazed joints, as illustrated in Figure 19, have shown practically no evidence of a secondary phase.

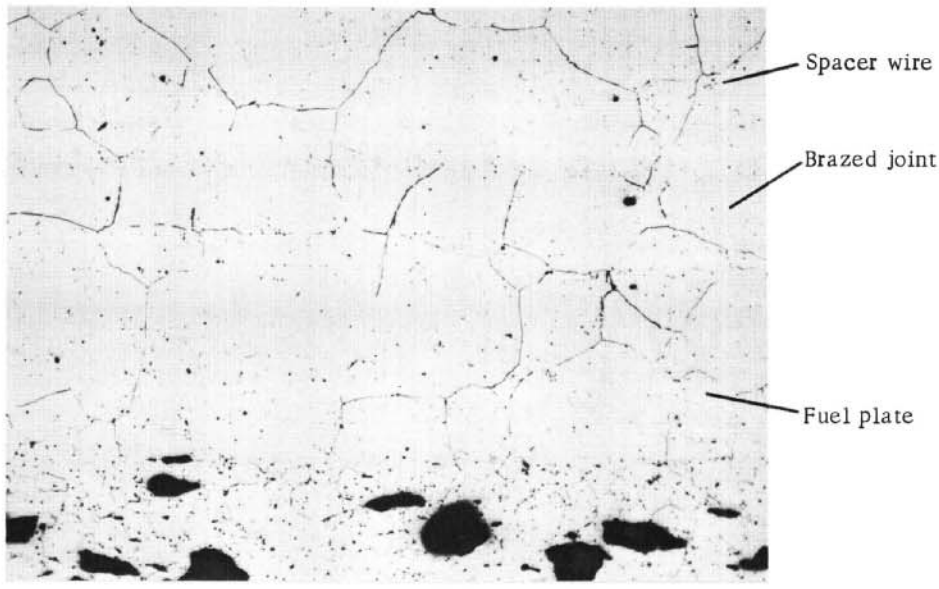

Micro 33365 150X

19a. Spacer-wire-to-fuel-plate joint

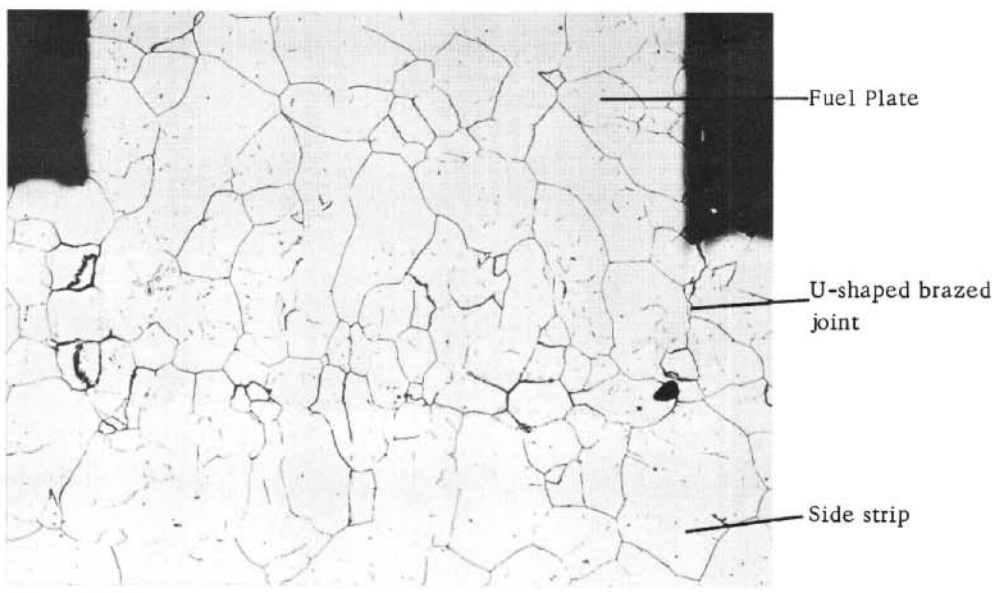

Micro 28265 100X

19b. Side-strip-to-fuel-plate joint

Figure 19. Typical Coast Metals 60 Brazed Fuel-subassembly Joints

Extensive examination of brazed, depleted fuel subassemblies was carried out to establish the dependability of the assembly procedures. It was initially found that the brazing alloy flowed quite freely over the fuel-plate surfaces and was therefore not sufficiently concentrated at the

desired locations (i.e., the spacer-wire-to-plate and side-strip-to-plate joints) to bridge fully the gap between the adjoining subassembly components. A large number of unbonded areas were found scattered throughout the developmental subassemblies.

It was determined that the extent of flow of the braze alloy was affected by the condition of the fuel-plate surfaces. Plate surfaces were prepared by sand blasting, vapor blasting, emery-cloth abrasion, and wire brushing. The most effective limiting of alloy flow was accomplished by wire brushing wherein very shallow [0.0025 mm (0.0001 in.)] longitudinal scratches are impressed onto the fuel plate surfaces. The use of stainless steel wire brushes in this part of the assembly procedure markedly improved the reproducibility of satisfactory brazing. Minor porosity, as seen in Figure 20, was still found at random locations, so elimination of porosity was not always complete. Since side-strip-to-fuel-plate brazed joints did not cover the core area of the plate, porosity at these joints was not as undesirable as at spacer-wire-to-fuel plate brazed joints. Most porosity was found at side-strip joints.

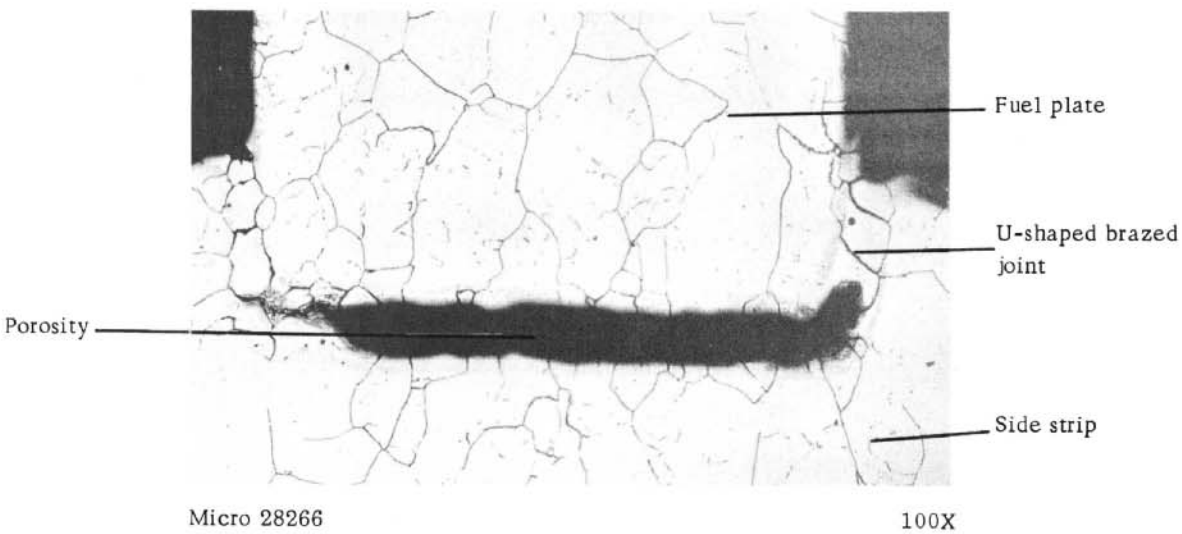

Figure 20. Brazed-joint Porosity

Some sections of brazed dummy subassemblies were tested in oxygenated steam (650°C, 42.2 kg/cm^2, 19-25 ppm O_2) for 37 days. After 4 days of exposure, tested sections were covered with a loose scale, as shown in Figure 21a. The amount of loose scale produced during subsequent exposure was greatly reduced, and an adherent film formed on the fuel-plate surfaces, as indicated in Figure 21b.* The Coast Metals 60 brazed joints appear sound

*In order to secure satisfactory operation of a nuclear-powered steam superheater, the fuel cladding must withstand high-temperature (500-700°C) steam containing oxygen and hydrogen. However, both significant general corrosion and cracking tendencies have been observed for 304 stainless steel in oxygenated steam.[16,17] A program is in progress at ANL to survey the general corrosion behavior of this material over a range of temperature (550-650°C) and of steam velocity (0-914 m/sec). Tests performed at 650°C and 42.2-kg/cm^2 gage have indicated that the corrosion behavior of the 18-8 series stainless steels is extremely sensitive to surface preparation under these temperature and pressure conditions.[17]

in these subassembly sections after corrosion testing. Separate Coast Metals 60 brazed samples of 304 stainless steel were tested in low-oxygen steam at 540°C and 42.2 kg/cm^2 for 147 days, and at 650°C and 42.2 kg/cm^2 for 93 days. Visual observation showed no signs of deterioration of the braze.

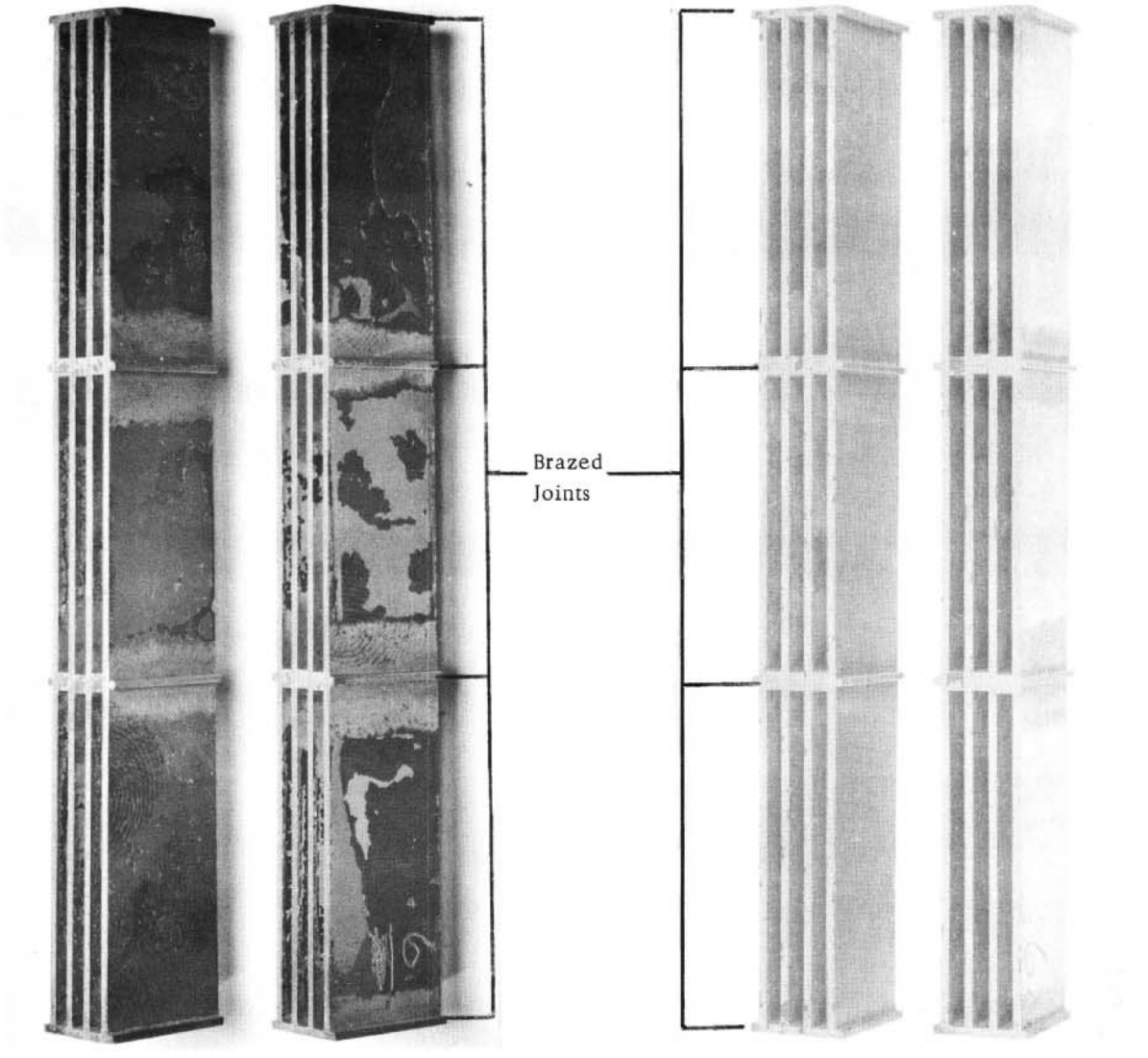

Macro 33506 1.5X

21a. After 4 days of exposure

Macro 33704 1.5X

21b. After 37 days of exposure

Figure 21. Brazed (Coast Metals 60) Depleted Fuel-subassembly Sections after Corrosion Testing in 650°C, 42.2 kg/cm^2 (600 psi), Oxygenated Steam

Subassembly Brazing

The brazing of fuel subassemblies followed the steps shown in Figure 1. A brazed subassembly consisted of four plates, each separated

by two 0.159-cm (0.0625-in.) square stainless steel spacer wires on 2.86-cm (1.125-in.) centers and supported at the edges by stainless steel comb-type side strips, as shown in Figure 22. Two stainless steel wires, of 0.79-mm (0.031-in.) diameter, on 2.86-cm (1.125-in.) centers, were also brazed onto the two outer plate surfaces. These wires provided spacing between the subassembly and an insulating envelope which fit around it. The square (inner spacer) wires were of the same length as the fuel plates, 61.6 cm (24.25 in.). The round (outer spacer) wires, 61 cm (24 in.) long, were flush with one end of the subassembly and run to within 0.6 cm (0.25 in.) of the other end of the subassembly. A 0.6-cm (0.25-in.) wide x 0.79-mm (0.031-in.) thick x 9.22-cm (3.630-in.) long stainless steel strip was also brazed onto the outer two subassembly plate surfaces at one end. This strip facilitated welding of an insulating can to the subassembly, as is described later in this report. The components for one subassembly are shown in Figure 23.

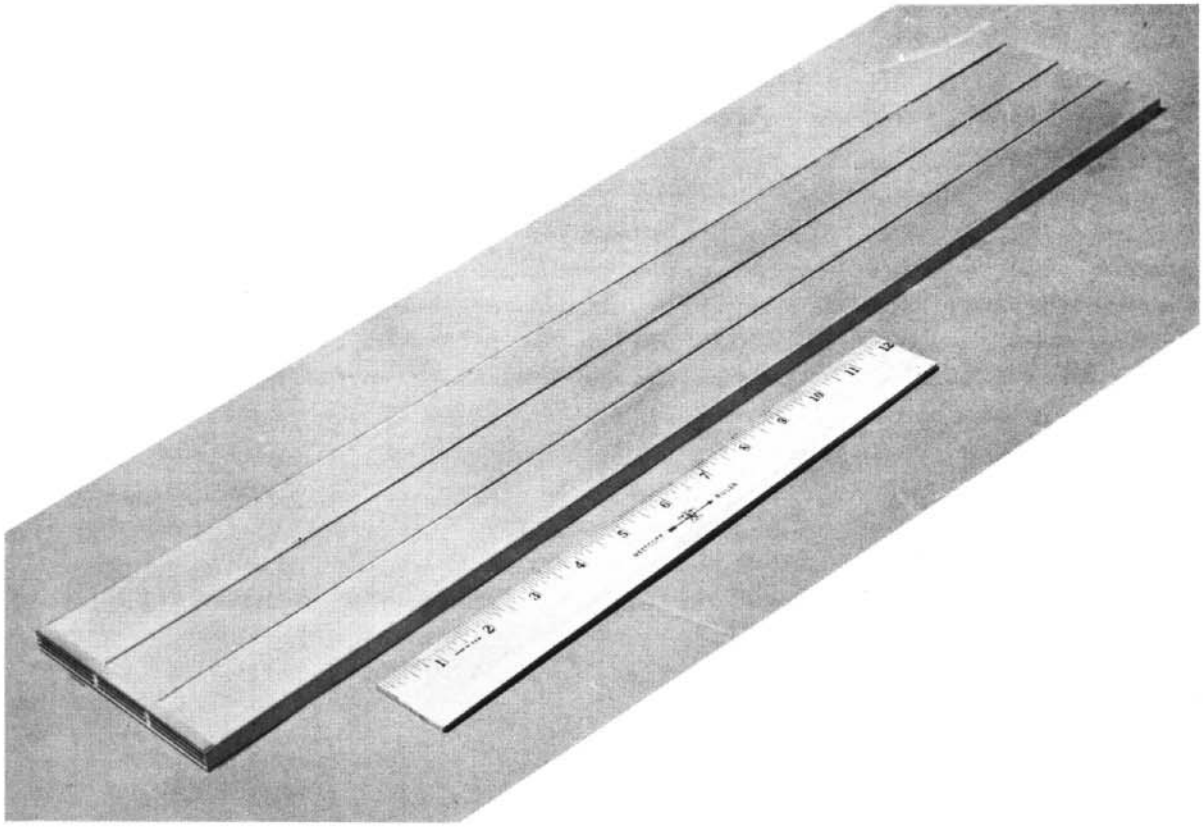

Figure 22. Brazed Fuel Subassembly

Fuel-plate surfaces were manually wire brushed in the longitudinal direction, and all subassembly components were cleaned in isopropyl alcohol prior to assembly. As discussed earlier, accurate alignment during assembly was insured by first tacking the wires to the plates at 7.78-cm (3.0625-in.) intervals with a condenser-discharge type of weld. A non-current-conducting (Micarta) holder, as shown in Figure 24, positioned both wires and plates during tack welding. After the holder was bolted

together, copper electrodes were inserted in holes in the top half of the holder. The locations of the holes were such that the electrodes contacted the 0.16-cm (0.0625-in.) square land areas on the square spacer wires. It was not found necessary to coin the round spacer wires.

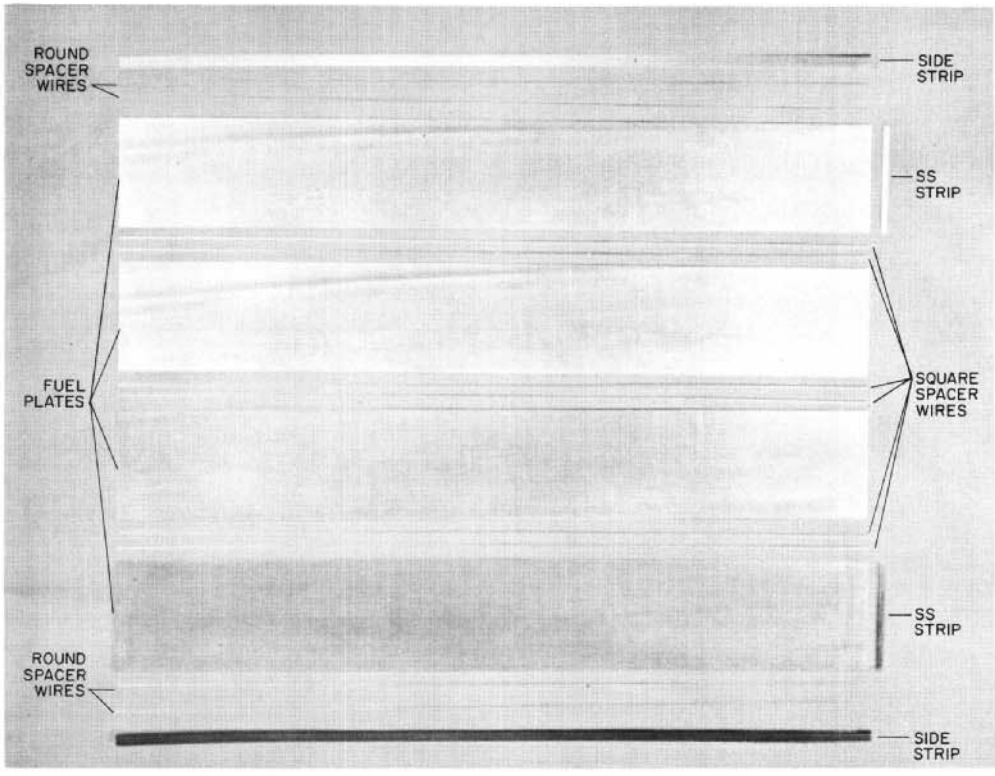

Figure 23. Fuel-subassembly Components

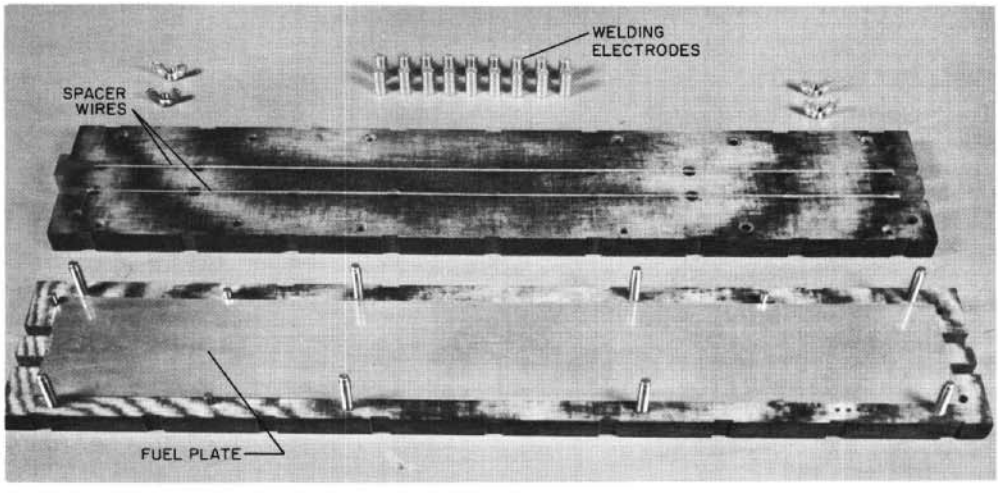

Figure 24. Fixture for Holding Fuel Plates and Spacer Wires during Tack Welding

Two welds were made simultaneously by circuiting the current between two electrodes on the same side of the plate. A record of gun pressure and amperage was maintained for all welds by a dual-pen strip-chart recorder, as illustrated in Figure 25. Welding parameters kept constant throughout the assembly period were: (a) capacitance (120 μf), (b) voltage (2000 V), and (c) gun pressure (38.6 kg). The cross section through a typical weld shown in Figure 26 confirms that tacking is achieved without overheating.

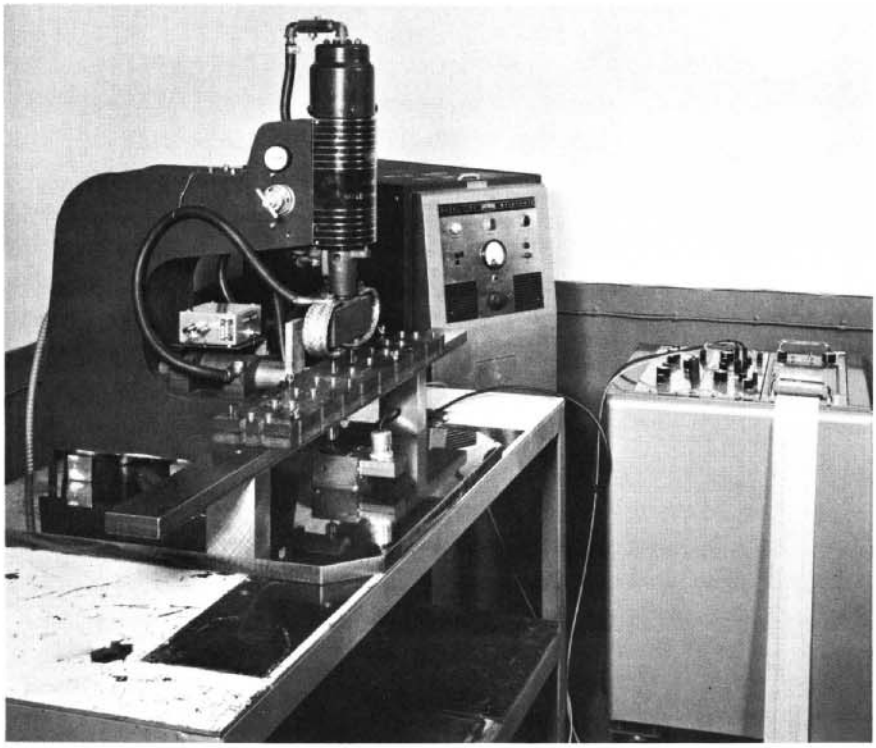

Figure 25. Tack-welding Equipment and Dual-pen Recorder

The fixtures used to support and contain the fuel subassemblies during furnace brazing are shown in Figure 27. The plates were assembled for brazing in a plate holder of heavy stainless steel. Dovetailed slots were machined into the holder to accept alumina wafers, which prevented diffusion bonding between the holder and the fuel plates during brazing. The method of assembly consisted of placing the comb-type side strips in the holder and slipping the fuel plates with spacer wires attached into the grooves in the side strips, as illustrated in Figure 28. As each plate was positioned, Coast Metals 60 brazing alloy was applied at all spacer-wire-to-plate and side-strip-to-plate joints. A hypodermic syringe was used to obtain a controlled application of braze material, as seen in Figure 29. A 40 v/o polystyrene-60 v/o benzene cement was used as carrier for the alloy in order to avoid chloride contamination from the more commonly used, chlorinated hydrocarbon cements. A corrugated stainless steel spacer was positioned alongside the assembled plates in the holder to facilitate removal of the subassembly after brazing. Alumina wafers were placed

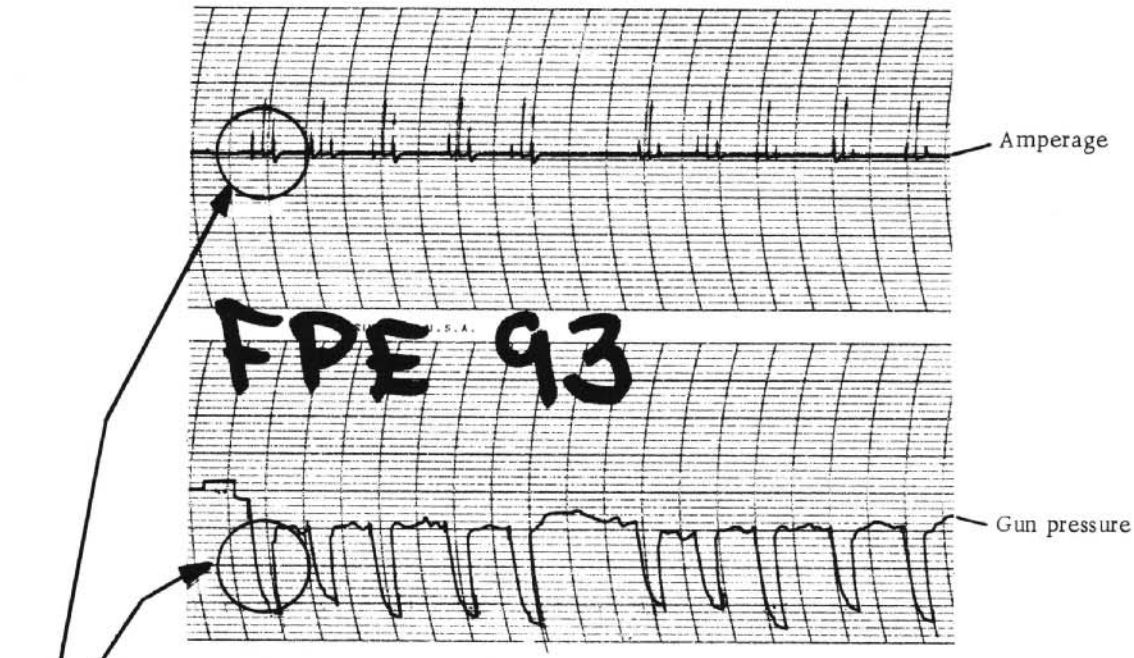

26a. Amperage and gun pressure recorded for plate FPE 93. These parameters were similarly recorded for all 10 welds on each fuel plate. (Chart units arbitrary.)

One Weld

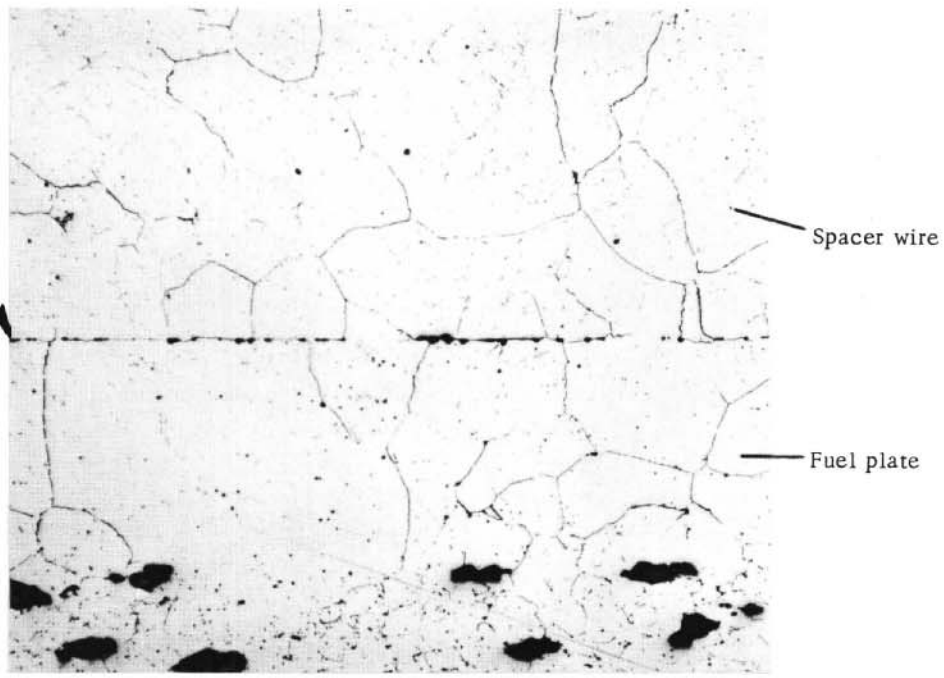

Micro 33364 150X

26b. Spacer wire to fuel-plate tack weld

Figure 26. Typical Dual Recording and Tack Weld between Spacer Wire and Fuel Plate

between the corrugated spacer and the subassembly side strip. Complete seating of the fuel plates into the side grooves was ensured by manually driving pieces of steel shim stock between the corrugated strip and the adjacent plate holder side after loading.

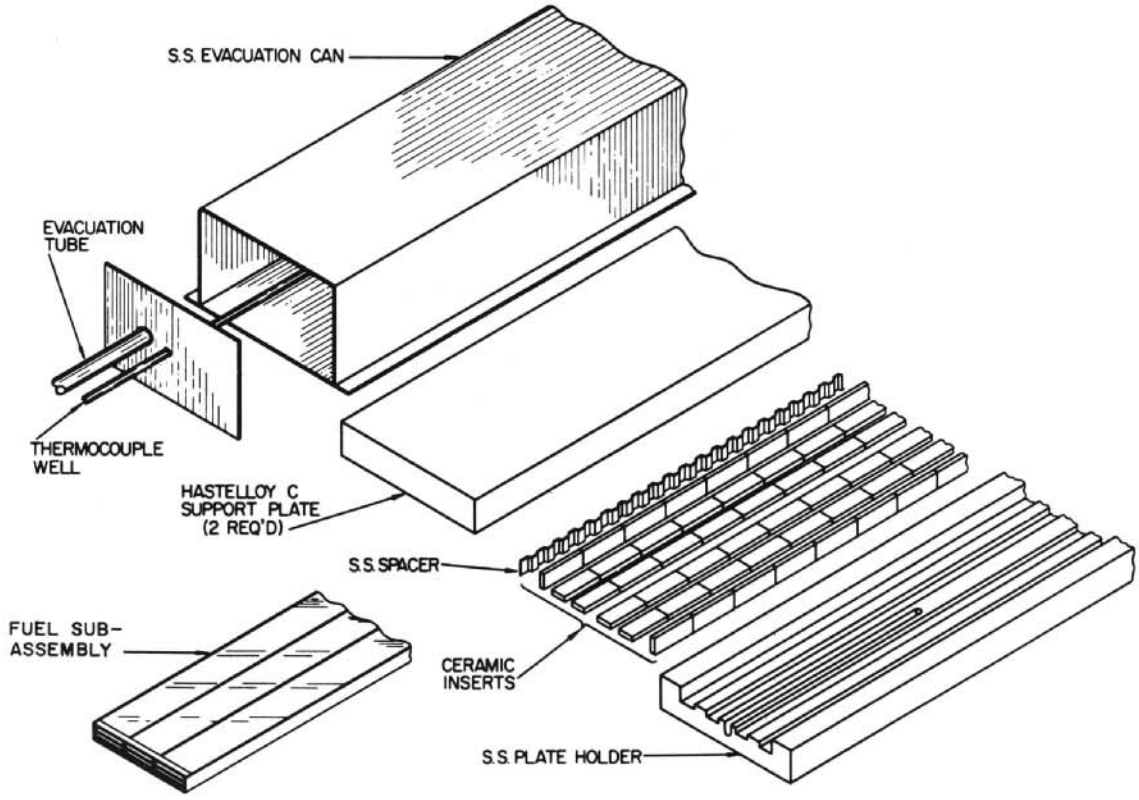

Figure 27. Contents of Evacuation Can during Vacuum Brazing of BORAX-V Superheat Fuel Subassemblies

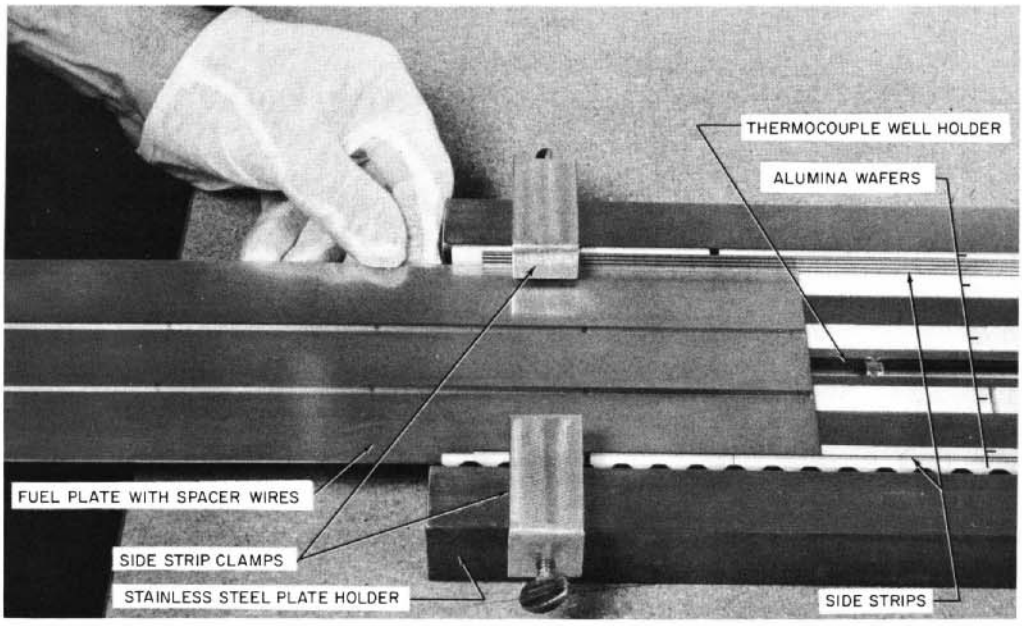

Figure 28. Slipping Fuel Plate into Side Strip Grooves in Plate Holder

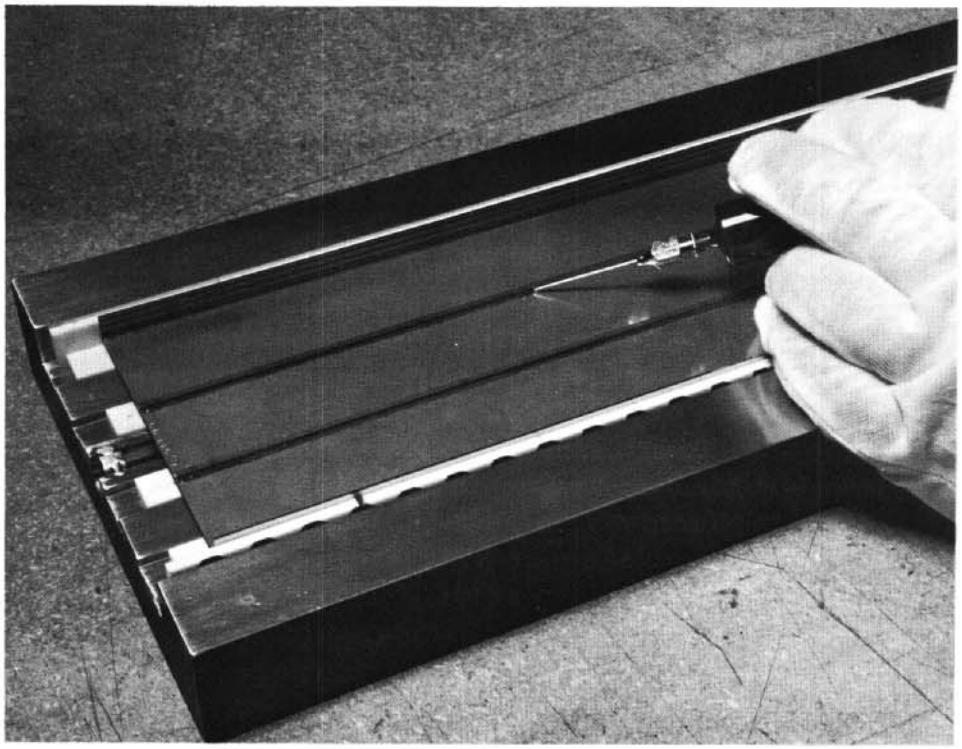

Figure 29. Application of Brazing Alloy at Spacer Wire-to-plate Joint

The plate holder was next sandwiched between Hastelloy-C plates, 2.5 cm (1 in.) thick, to support the stainless steel holder and prevent thermal distortion of the subassembly. The Hastelloy-C support plates were flame sprayed with an alumina coating to prevent diffusion bonding. The top Hastelloy-C support plates were eventually fitted with dovetail slots and alumina wafers to eliminate the need for repeated flame spraying. (Figure 27 does not show the Hastelloy-C support plates so fitted.)

The entire fixture was then inverted to aid flowing of the braze alloy into the spaces between each spacer wire and both fuel plates contiguous to the wire. Inverting the fixture also aided complete filling of all side-strip grooves. The inverted assembly was inserted in a 0.13-cm (0.050-in.) thick stainless steel evacuation can. A cover plate with attached evacuation tube and sealed thermocouple well was then fitted to the can and heliarc welded to it. The sealed can was checked for leaks with a mass-spectrometer helium leak detector. Five subassemblies were brazed simultaneously by heating to 1160°C in two air-atmosphere silicon carbide resistance furnaces, as shown in Figure 30. Evacuating the steel cans to a pressure of 1×10^{-3} torr or less caused the thin-walled cans to collapse onto the Hastelloy-C supports and the stainless steel holders. In this way, a uniform constant pressure of approximately 1 atm was maintained on the components throughout the brazing cycle. Following a 2-hr soak period at the brazing temperature, the refractory bricks were

partially removed from the furnace doors. Furnace cooling to approximately 500°C was accelerated somewhat by directing fan-driven air currents at the open furnaces. A complete record of temperature and vacuum conditions was maintained for each subassembly throughout the 16-hr brazing cycle. Table XI is a tabulation of typical cycle conditions. Figure 31 is a graphic presentation of pressure and temperature versus time.

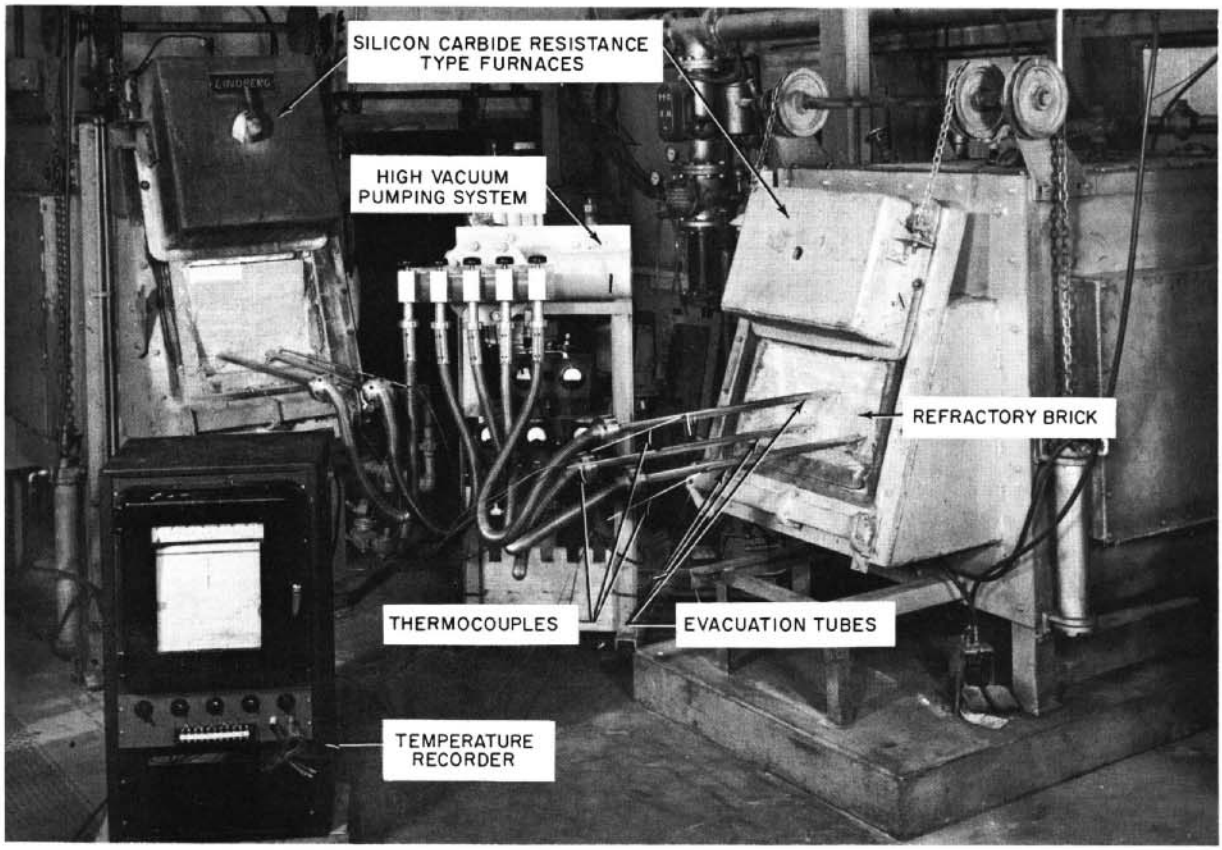

Figure 30. Equipment for Vacuum-brazing Fuel Subassemblies

Table XI

TYPICAL TEMPERATURE AND PRESSURE CONDITIONS DURING BRAZING CYCLE

Time	Pressure (torr)	Evacuation Can Thermocouple Readings (°C)					Time	Pressure (torr)	Evacuation Can Thermocouple Readings (°C)				
		1	2	3	4	5			1	2	3	4	5
0805	Evacuation begun	-	-	-	-	-	1700	2×10^{-4}	1083	1072	1080	1083	1104
0845	3×10^{-5}	Power on					1730	8.6×10^{-5}	992	986	1038	1012	1038
1030	3×10^{-4}	182	178	212	428	212	1800	6×10^{-5}	901	898	966	890	966
1100	3×10^{-4}	357	388	414	585	429	1830	4.6×10^{-5}	846	841	921	872	921
1130	2.6×10^{-5}	514	532	550	749	543	1900	3.6×10^{-5}	788	788	869	846	869
1200	2.2×10^{-5}	696	718	740	897	730	1930	2.4×10^{-5}	742	737	822	802	822
1245	3×10^{-5}	891	906	931	1001	927	2000	2.4×10^{-5}	720	716	802	780	797
1315	5×10^{-5}	991	997	994	1024	994	2030	2.4×10^{-5}	687	685	773	754	771
1345	2×10^{-4}	1074	1074	1074	1112	1074	2100	2.2×10^{-5}	649	644	735	716	733
1415	3×10^{-4}	1133	1133	1139	1148	1139	2130	1.9×10^{-5}	625	621	716	696	711
1430	4×10^{-4}	1157	1160	1160	1163	1160	2200	1.8×10^{-5}	597	592	687	670	683
1500	4×10^{-4}	1163	1163	1163	1166	1163	2230	1.6×10^{-5}	572	569	666	651	663
1530	4×10^{-4}	1163	1163	1164	1164	1163	2300	1.5×10^{-5}	546	543	642	630	640
1600	3.6×10^{-4}	1163	1161	1163	1163	1163	2330	1.3×10^{-5}	508	506	608	604	604
1630	3.6×10^{-4}	1163	1160	1163	1163	1163	2400	1.0×10^{-5}	492	487	592	592	588

Evacuation Cans Removed from Furnace.

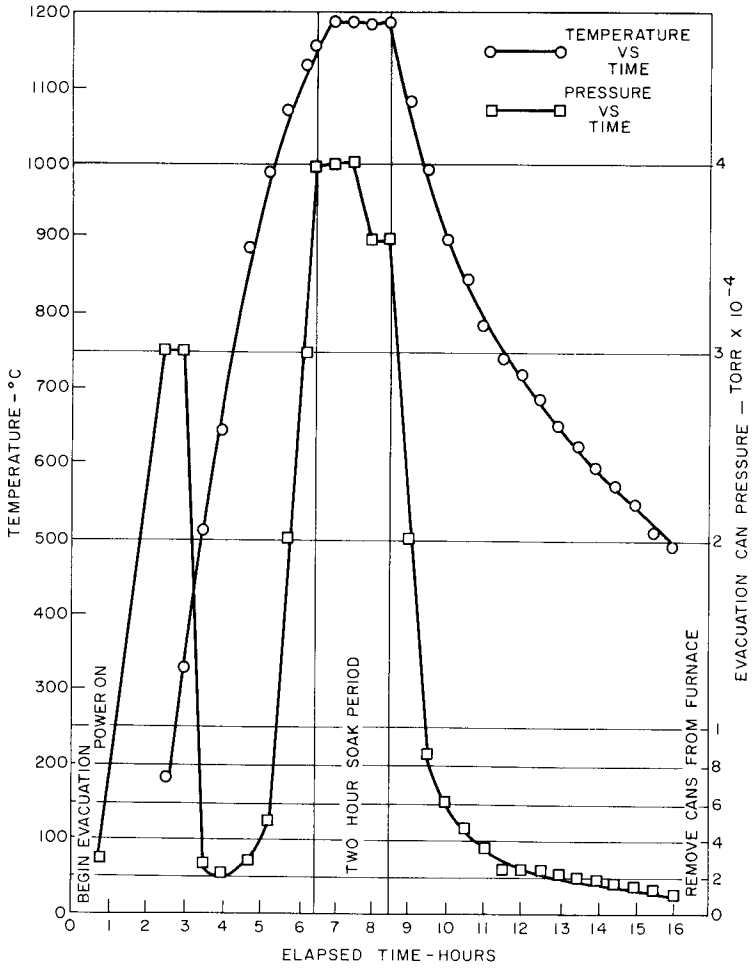

Figure 31. Chart of Temperature and Pressure Conditions during a Typical Brazing Cycle

The assembly and brazing of instrumented subassemblies was done in basically the same way as described above for the standard subassemblies. Several additional steps were required, however. Instrumented subassemblies were fitted with either six or eight thermocouples. Figure 32 is a perspective drawing of an instrumented subassembly with eight thermocouples. The chromel-alumel thermocouples were of 0.10-cm (0.040-in.) diameter with stainless steel sheaths. The sensing ends of the thermocouples, flattened to 0.18 cm x 0.05 cm (0.070 in. x 0.020 in.), entered through the subassembly side pockets and were brazed into 0.6-cm (0.25-in.) deep x 0.22-cm (0.085-in.) long x 0.06-cm (0.025-in.) wide pockets opening to the edges of the fuel plates. Since plate side cladding ranges from 0.15 cm (0.060 in.) to 0.28 cm (0.110 in.) in width, the thermocouple tips, when in the 0.6-cm (0.25-in.) deep pockets, will be measuring temperatures well within the plate cores. The pocket depth is more than 8 times greater than the plate thickness of 0.64 cm (0.030 in.). Heat dissipated to the plate edge from the thermocouple tip location should therefore

be negligible in comparison with heat loss to the fuel plate surfaces. Fuel-center temperatures are therefore expected to be accurately measured.

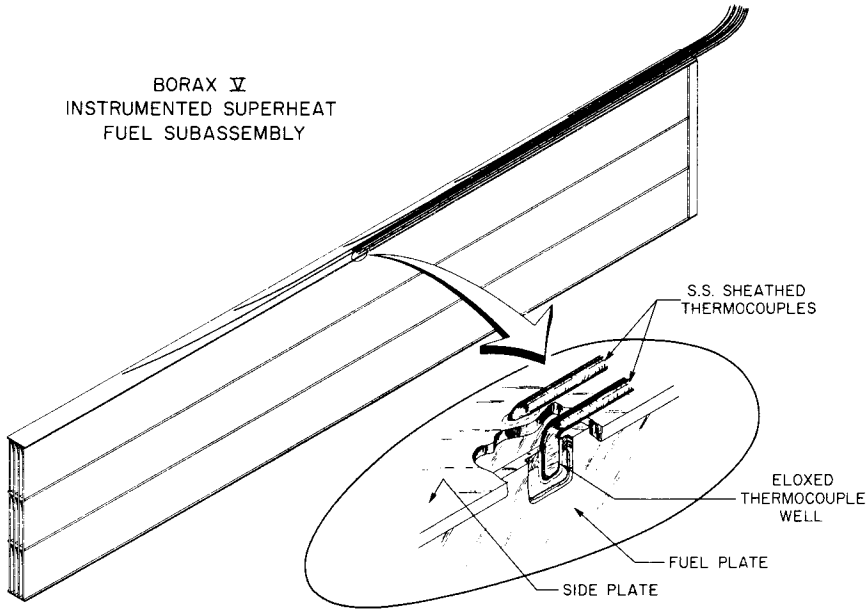

Figure 32. BORAX-V Instrumented Superheat Fuel Subassembly

The pockets were made in the plates by electrical discharge machining 0.38-mm (0.015-in.) wide slots starting from the plate edges and expanding the slots to the 0.6-mm (0.025-in.) width with a manually driven wedge. The plates are so thin that the electrical-discharge machining operation had to be closely controlled to prevent deviation of the pocket toward either of the plate surfaces. Even with the exercise of extreme caution, 10 plates had to be scrapped because of defectively machined pockets.

Some Coast Metals 60 was injected into the pocket before positioning of the thermocouple tip. After the thermocouple was inserted, the remainder of the pocket was filled with alloy. Additional brazing alloy was applied to bond the thermocouple sheaths to the subassembly side strips. All instrumented subassembly components were assembled with the use of special clamping devices, and the entire subassembly as a unit was then placed into the plate holder to position thermocouples along one side strip of the subassembly. Instrumented subassemblies were brazed in a vertical position with the electrical-discharge machined (Eloxed*) pockets upward to reduce any tendency for the brazing material to flow out of the pockets. Nine instrumented central and six instrumented peripheral subassemblies were brazed.

*Elox: trade name of electrical-discharge machine manufactured by the Elox Corporation, Royal Oak, Michigan.

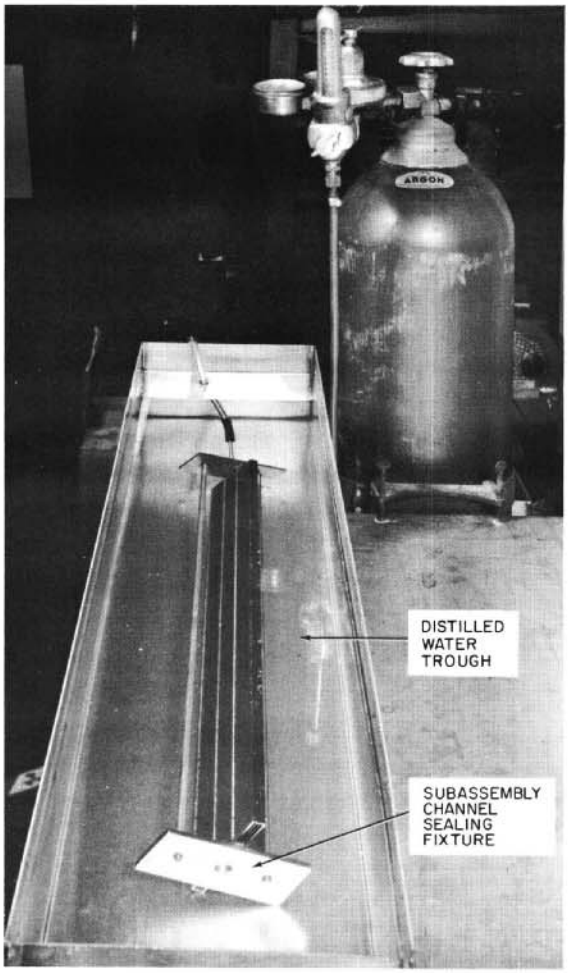

Figure 33. Leak-testing a Brazed Subassembly

Evacuation cans were stripped away after the brazing operation by grinding free the welded can closure and shearing off welded strips along both sides of the can.

Each subassembly was tested for possible leakage of gas at all mating interfaces. The leak test consisted of sealing the ends of the steam coolant channels, introducing argon gas under 1.4-kg/cm^2 gage (20 psig) through a calibrated hypodermic needle into the sealed channels, and observing any leakage of gas from between spacer wires and fuel plates or side strips and fuel plates, while the subassembly was immersed in distilled water, as illustrated in Figure 33. The size of each leak was determined by trapping all gas escaping from the leak in one minute and comparing the volume of trapped gas with the total volume of gas which could flow through the calibrated needle in the same length of time. Argon under 1.4-kg/cm^2 gage (20 psig) flowed through a No. 21 needle, with an opening of 2.3 x 10^{-3}/cm^2 (3.5 x 10^{-4} sq in.), at the rate of 2800 cc/min. A leak rate exceeding 1400 cc/min was arbitrarily established as being large enough to warrant rebrazing of the subassembly.

Rebrazing required application of additional brazing alloy at the location of leakage and repeating the canning, evacuating, heating, and cooling cycle as described above. A total of 6 central type and 23 peripheral type subassemblies were rebrazed. All subassemblies were found acceptable after rebrazing with one exception. A peripheral subassembly was rebrazed 3 times with no effective sealage of leaks occurring. This subassembly was not used in a reactor element.

Completion of Elements

The major steps involved in completing the BORAX-V superheat fuel elements, as outlined in Figure 1, were straightforward and required only a minor amount of procedural development. Views of a fuel element at three stages of assembly are shown in Figure 34. The operations involved in these final assembly stages are described below.

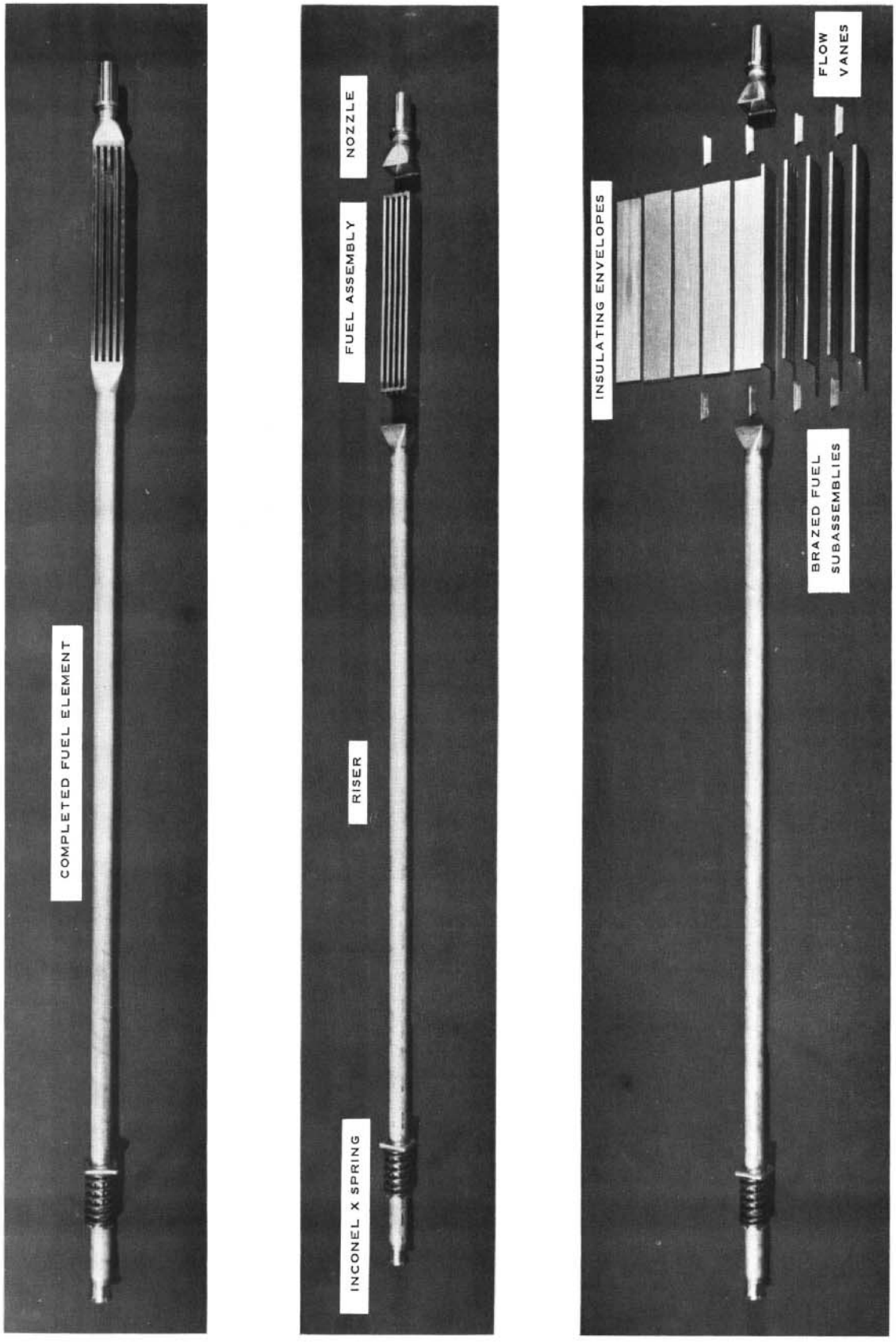

Figure 34. Exploded and Completed Views of a Fuel Element

To hold heat transfer between fuel subassemblies and insulating cans to a minimum, the side strips and outer round wire spacers on each subassembly were machined such that contact areas were 0.32 cm (0.125 in.) long and spaced 3.57 cm (1.406 in.) apart. Figure 35 shows a subassembly being machined. The depth of the machined areas (see Figure 36) was 0.32 mm (0.0125 in.). Two subassemblies were accidentally damaged during machining and could not be used. As part of the final dimensional inspection of the subassemblies, each steam-flow channel was plug gaged with a 1.3-cm (0.50-in.) wide x 0.14-cm (0.056-in.) thick plug.

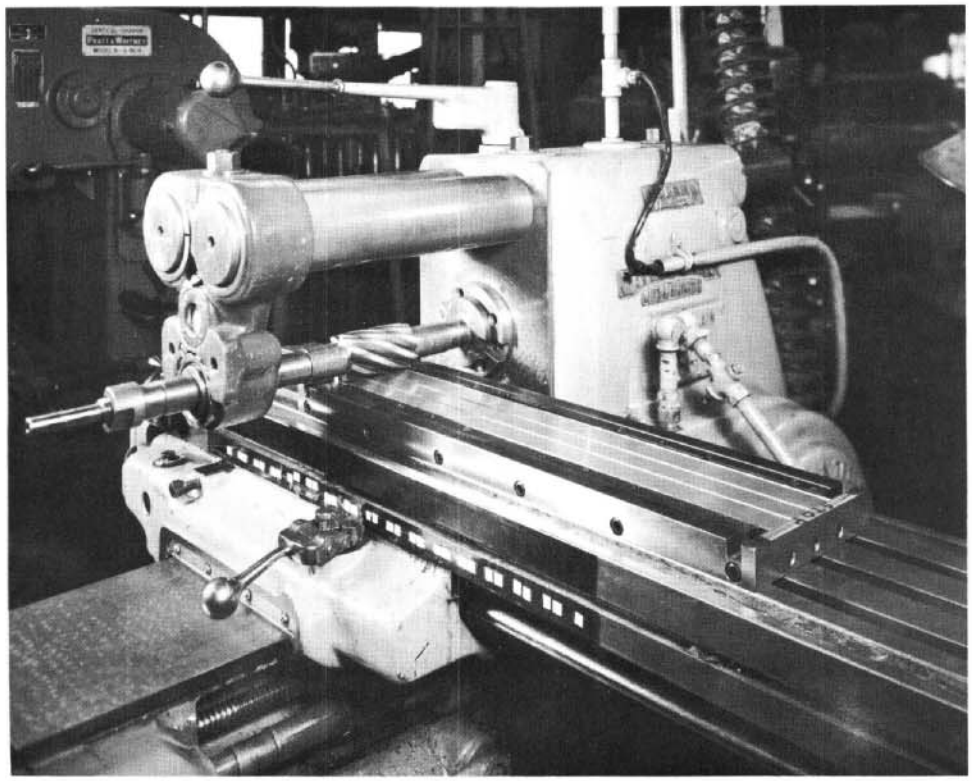

Figure 35. Machining Subassembly Side Strips and Outer Wire Spacers

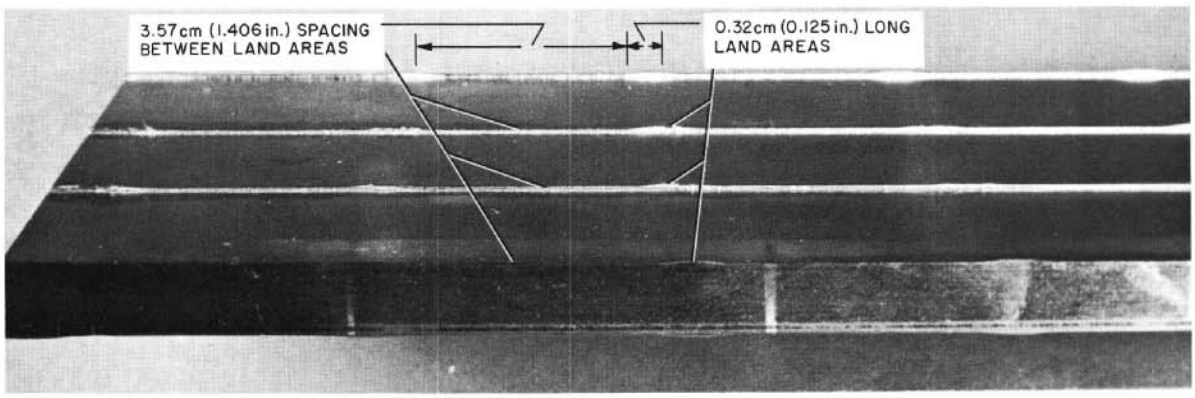

Figure 36. Fuel Subassembly after Machining

A fuel assembly, shown in Figure 37, consisted of 5 brazed subassemblies in insulating cans welded together with flow vanes at each end. Each brazed subassembly was slipped into a 0.8-mm (0.030-in.) thick rectangular, open-ended stainless steel insulating envelope. Each subassembly was centered within its insulating envelope so that a constant annular spacing was maintained between these two components. This rectangular spacing measured 0.16 cm (0.0625 in.) at the sides (between subassembly side strips and parallel insulating envelope sides), and 0.8 mm (0.031 in.) at both top and bottom (between subassembly outer fuel plate surfaces and parallel envelope sides). The raised portions of the machined outer round wire spacers and subassembly strips insured that this annular spacing was maintained at top and bottom. Insulating envelope sides were dimpled 0.16 cm (0.0625 in.) inward at one end to center the subassembly. At the other end, 0.16-cm (0.0625-in.) thick x 0.6-cm (0.25-in.) wide strips were inserted between envelope sides and side strips. These inserted strips and the two 0.8-mm (0.031-in.) thick x 0.6-cm (0.25-in.) wide strips brazed to top and bottom of the subassembly at this end completely filled the spacings between all four envelope sides and corresponding subassembly components.

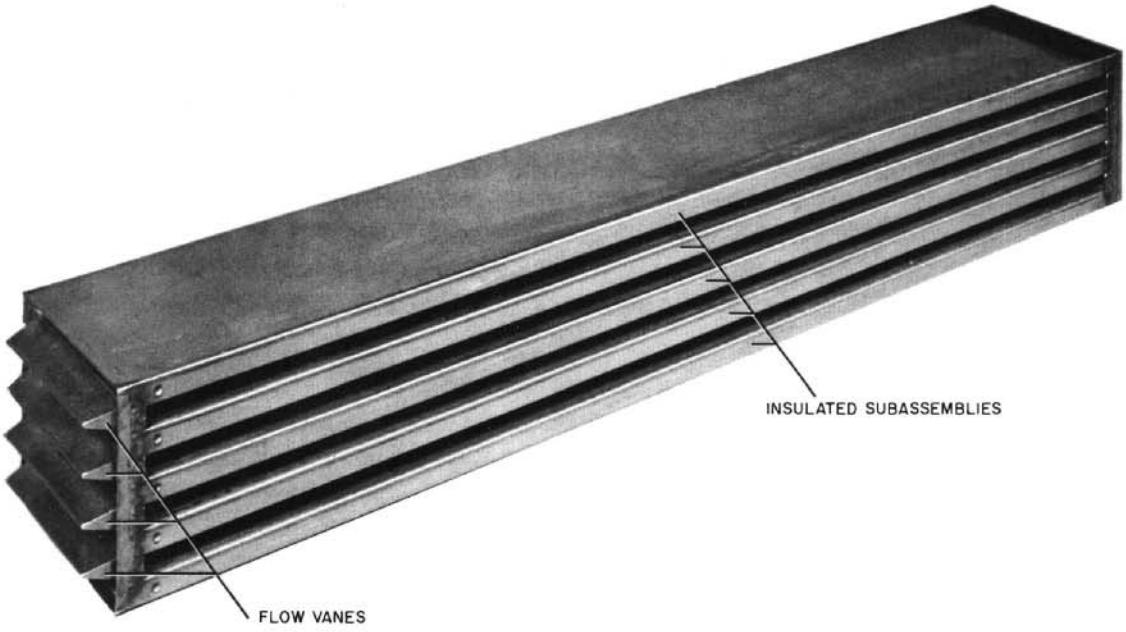

Figure 37. Completed Fuel Assembly

During the assembly welding operation, illustrated in Figure 38, heliarc welds were also applied to seal this spacing completely at one end of the insulated subassemblies. (Static steam will therefore surround each subassembly during reactor operation.) The assemblies were completed by heliarc welding the flow vanes to the insulating envelopes, at each end and between each subassembly, as seen in Figure 38. The flow vanes space each subassembly 0.94 cm (0.370 in.) apart so that completed

assemblies have a 9.30-cm x 9.84-cm (3.663-in. x 3.875-in.) cross section. Each fuel assembly is 68.6 cm (27 in.) long. The two ends of a fuel assembly, showing the spacings between subassemblies and insulating envelopes which are sealed by welding at one end, are shown in Figures 39a and 39b.

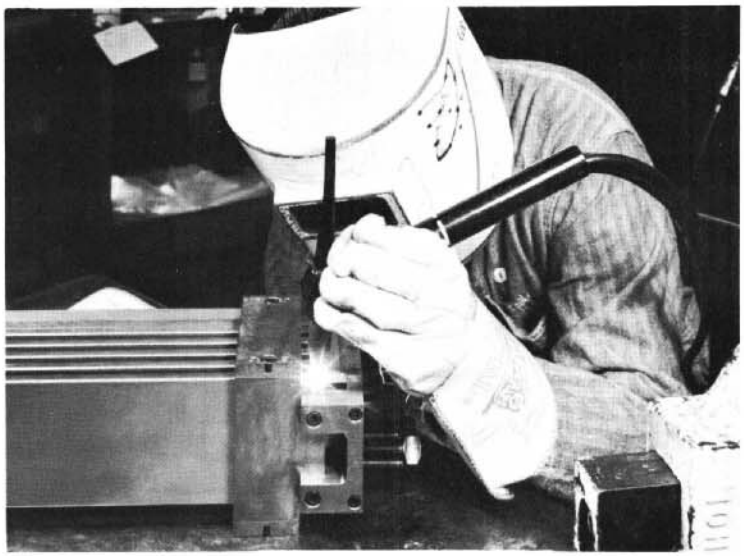

Figure 38

Heliarc Welding Fuel Assembly

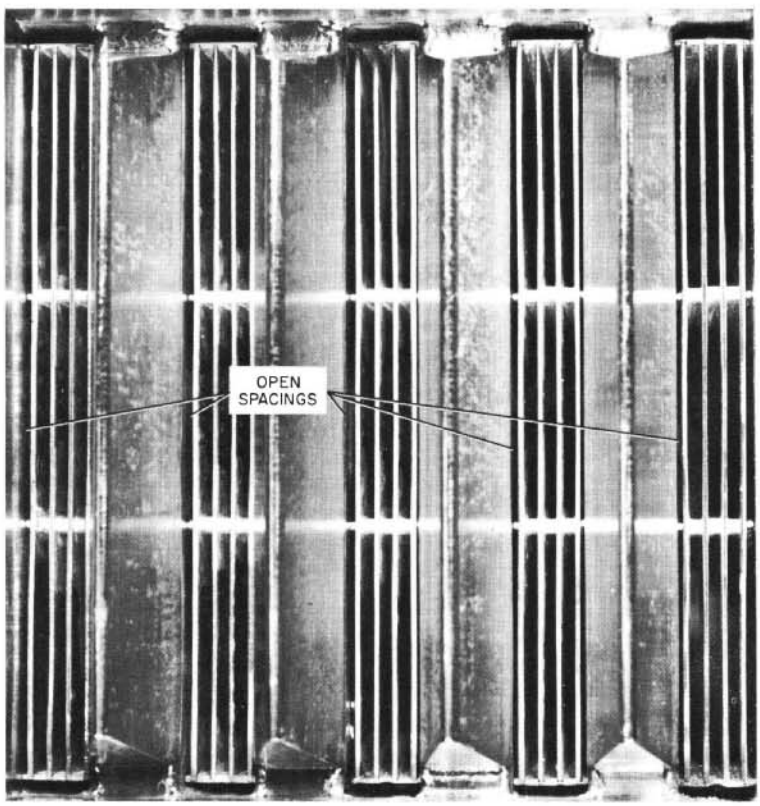

1X

Assembly end with open spacings between subassemblies and insulating cans

Figure 39a. End Views of a Fuel Assembly

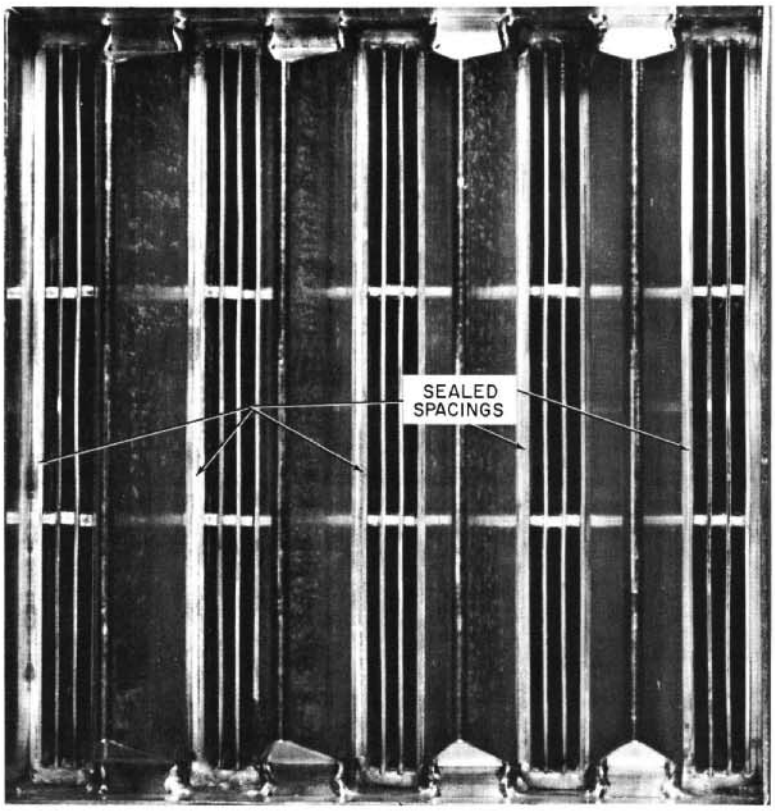

1X

Assembly end with sealed spacings between subassemblies and insulating cans

Figure 39b. End Views of a Fuel Assembly

Instrumented fuel assemblies have 20 thermocouples to measure temperatures within individual fuel plates. Of the five subassemblies comprising an instrumented assembly, 2 subassemblies are fitted with 6 thermocouples each and 1 subassembly has 8 thermocouples. All 5 instrumented assemblies were fitted in this fashion.

A fuel assembly, with riser and nozzle heliarc welded to its respective ends, comprises a final fuel element. The transition pieces of 304 SS were commercially fabricated.

Although all nozzles are identical, risers differ in two ways. In every case, nozzles are about 25.4 cm (10 in.) long. Risers, however, due to varying lengths of riser tube, are of three different overall lengths. All nozzles contain inner liners to act as thermal insulation, whereas some risers do and some do not contain inner liners. Varying riser lengths were made necessary due to the geometry of the BORAX-V reactor vessel. The reason that not all risers required liners can best be given by describing the steam-flow path through the superheat fuel elements.

The superheat loadings (central and peripheral) were designed so that saturated steam from the boiling section of the reactor core will flow down through one superheat fuel element and up through a second superheat fuel element before leaving the reactor vessel. The saturated steam will first enter the inlet riser of an inlet fuel element, flow down through the fuel assembly section, and out the lower nozzle. This partially superheated steam will then enter the nozzle of an outlet fuel element, flow up through the assembly section, and out the outlet riser. All nozzles and outlet risers contain liners to thermally insulate the superheated steam. Inlet risers do not contain liners, because steam entering them is not superheated.

Inlet elements are either 3.81 m (12 ft 6 in.) (designated standard) or 3.76 m (12 ft 4 in.) (designated short), depending on the lengths of their risers. Outlet elements have shorter risers and are 3.71 m (12 ft 2 in.) in length. A 15.2-cm (6-in.) long Inconel X spring of 1.43-cm (0.562-in.) diameter wire is fitted around each riser tube at its upper end. This spring acts to effect a nozzle O-ring-to-steam plenum seal during reactor operation.

Instrumented elements are the same length, 3.71 m (12 ft 2 in.) and similar in construction to outlet fuel elements. Each instrumented element, as previously discussed, has 20 thermocouples brazed into pockets machined in fuel plates. In addition, the tips of two thermocouples, entering through holes in the center flow vane, are positioned such that the temperature of the partially superheated steam, flowing through the fuel element nozzle, will be measured immediately before entering the assembly portion of the element. Outlet (fully superheated) steam temperature will be measured by two more thermocouples with sensing ends inserted in an axial hole in a 0.6-cm (0.25-in.) diameter cross bar, inside, and welded to, the riser tube wall about 10.2 cm (4 in.) from the fuel assembly. A venturi tube was mounted inside the riser tube to measure steam flow velocity. The venturi tube is located about 1.22 m (4 ft) down from the top of each instrumented fuel element riser.

ASSEMBLY SUMMARY

Figure 40 summarizes the assembly of BORAX-V superheat fuel elements. Fuel plates containing four different amounts of UO_2 were used in fabricating the brazed subassemblies. Outside plates of each four parallel-plate subassembly were fabricated with about one-half the amount of UO_2 contained in the inner plates. In central-type subassemblies, outer plates are designated Half Central Enriched (HCE) and inner plates are designated Full Central Enriched (FCE). Half Peripheral Enriched (HPE) and Full Peripheral Enriched (FPE) are the corresponding designations for plates in peripheral type subassemblies. The total amount of UO_2 contained in a peripheral subassembly was approximately $1\frac{1}{2}$ times the amount contained in a central subassembly.

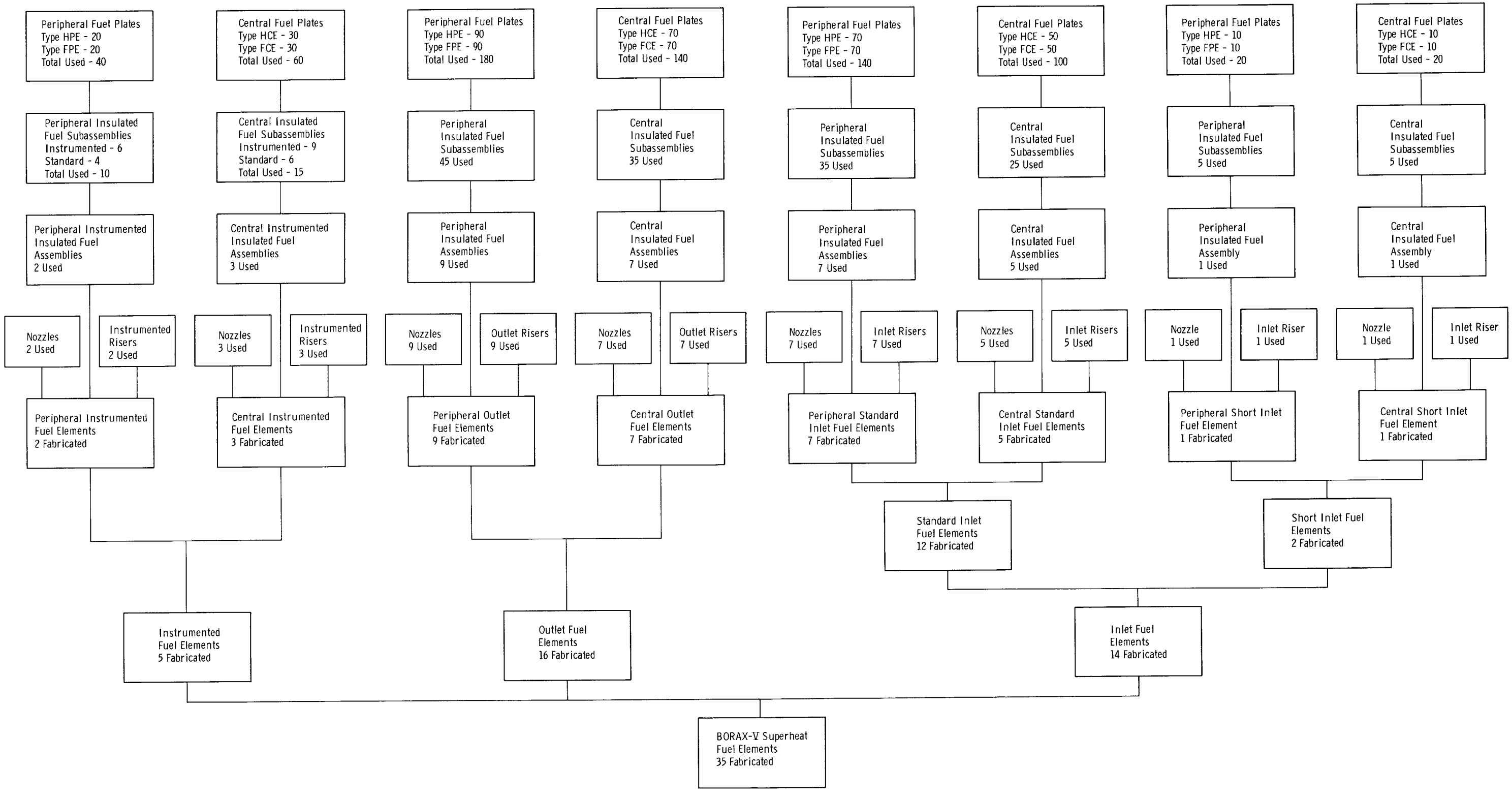

Figure 40. Fuel Element Assembly Summary

A development program was conducted before a dependable fuel-subassembly brazing procedure could be established. Strong, ductile joints were attained by using Coast Metals 60 brazing alloy, but the flow of the alloy had to be controlled. When this was accomplished, sound joints containing a minimum of porosity were reproducible with a high degree of reliability.

The fixtures built and used during subassembly brazing and remaining assembly operations were uniquely designed. For the most part, the remaining assembly operations presented no extraordinary development problems. An insulated subassembly has four fuel plates, brazed together in parallel, inside an open-ended stainless steel envelope. Each fuel assembly, whether peripheral or central, has five insulated subassemblies heliarc welded together in parallel with flow vanes at each end.

A fuel element consists of a fuel assembly with a riser and a nozzle attached, by heliarc welding, to its ends. All fuel assemblies and all nozzles are the same lengths. Risers, and the completed fuel elements, are of three different lengths. The central superheat loading is composed of 16 fuel elements: one short inlet, 3.76 m (12 ft 4 in.) long; five standard inlet, 3.81 m (12 ft 6 in.) long; seven outlet, 3.71 m (12 ft 2 in.) long; and three instrumented, 3.71 m (12 ft 2 in.) long. The peripheral superheat loading is composed of 19 fuel elements: one short inlet, seven standard inlet, nine outlet, and two instrumented. The total number of fuel elements fabricated for fueling the BORAX-V superheater was 35.

CONCLUSIONS

The commercial fabrication of fuel plates for BORAX-V superheat fuel elements was successfully accomplished. Although the first plates fabricated departed significantly from specifications, the vendor cooperated to the fullest possible extent in revising fabrication procedures to correct these discrepancies. The resultant fuel plates were markedly improved and of a quality which correlates quite closely with specifications. The attributes that these plates possess are as nearly optimized as can be expected within the current state of dispersion fuel-fabrication technology.

Vacuum-furnace brazing was developed as the fuel-assembly method. The joints attained with a Cr-Fe-Ni-Si (Coast Metals 60) brazing alloy have good strength and ductility, and a minimum of porosity. Joining of all transition pieces to complete the fuel elements was done by heliarc welding.

The core with a central superheater was loaded into BORAX-V during April, 1963. After operation with this configuration, the core will be removed and replaced with the core having a peripheral superheater. Peripheral superheat fuel elements are being stored at the Laboratory's DuPage site until needed sometime during calendar year 1964.

FUTURE PLANS

Work is currently progressing at ANL on two other projects associated with BORAX-V superheat fuel. Type 406 SS has demonstrated corrosion resistance superior to Type 304 SS under test conditions simulating those anticipated in the BORAX-V superheat core. As a further test of this material for nuclear superheat use, two central superheat fuel elements are being fabricated with fuel plates clad with Type 406 SS. These elements will be inserted in the core with central superheater for operation along with the Type 304 SS-clad fuel.

The other project has to do with development of improved cladding materials and fabrication procedures for superheat fuel elements of two advanced designs. One element concept would utilize spherical fuel pellets consisting of UO_2 balls of 0.90-cm (0.355-in.) diameter encapsulated in 0.25-mm (0.010-in.) thick cladding.

The second fuel design concept consists of pea-in-a-pod-type fuel rods. This nomenclature is meant to describe the fuel-rod geometry which results when tubing with a 0.25-mm (0.010-in.) thick wall, and filled with 0.82-cm (0.321-in.) diameter UO_2 balls, is collapsed or formed inward around the balls. Promising candidate materials for superheat fuel are being evaluated. Until a superior cladding material is found, development of forming and joining techniques for 406 SS will be primarily emphasized.

ACKNOWLEDGEMENTS

The authors extend their appreciation to the many individuals who aided in the cooperative efforts required to complete the BORAX-V Superheat Fuel Elements.

F. G. Foote and R. E. Macherey provided the guidance necessary to see this project through to its completion.

The Central Shops Department deserves special recognition for the development of brazing procedures and the assembly of the BORAX-V Superheat Fuel. A. A. Denst, C. T. Szymko, H. W. Ostrander, and the men under them were responsible for assembly development and assembly operations. S. V. Smith was the foreman in charge of the special materials shop wherein the assembly work was performed. O. E. Layton was primarily responsible for the smoothness with which the overall scheduling and production planning was carried out.

We are indebted to the following members of the Foundry and Fabrication Group of the Metallurgy Division. R. D. McGowan was responsible for much of the evaluation of fuel plates and brazed fuel subassemblies.

The actual preparation of samples and gathering of data during destructive evaluation were performed by C. Steves, R. M. Hendrickson, D. L. Hoffman, R. M. Jedinak, and H. C. Glienke. J. A. Zic was in charge of record keeping and maintenance of criticality standards for the duration of evaluation and assembly operations.

The nondestructive evaluation of the fuel plates was ably performed by R. H. Selner, R. L. Irwin, and R. B. Perry of the Nondestructive Testing Group of the Metallurgy Division, and N. S. Beyer, B. F. Geren, and J. W. Tolle of Special Materials and Services Division.

R. W. Bane and R. E. Telford were especially cooperative in providing prompt precise analyses on plate core samples submitted to the Chemistry Division.

The photographs in this report were taken by L. E. Gorney of Graphic Arts. The prints of the photomicrographs were prepared by A. P. Baudino, Jr. of the Metallurgy Division.

The authors wish to thank Edna M. Bahr for her able preparation of the manuscript, and R. M. Mayfield for his assistance in editing the final manuscript.

REFERENCES

1. Design and Hazards Summary Report, Boiling Reactor Experiment (V) (BORAX-V), ANL-6302 (May 1961).

2. C. E. Weber, "Progress on Dispersion Elements," Progress In Nuclear Energy Series, V, Vol. 2, Metallurgy and Fuels (1959).

3. J. E. Cunningham, R. J. Beaver, R. D. Robertson, and E. C. Edgar, Specification and Fabrication Procedures for APPR-1 Core II Stationary Fuel Elements, ORNL-2649 (Feb 1959).

4. C. T. Armenoff and M. H. Binstock, Fuel Elements for the Organic Moderated Reactor Experiment, NAA-SR-1934 (Dec 1957).

5. S. D. Megeff and H. S. Kalish, Investigations on Stainless Steel-UO_2 Fuel Element Core Material, SEP-175 (Aug 1955).

6. R. J. Beaver, R. C. Waugh, C. F. Leitten, Jr., and W. R. Burt, Jr., Investigation of the Factors Affecting Sensitization of Army Package Power Reactor (APPR-1) Fuel Elements, ORNL-2312 (Oct 1957).

7. J. E. Cunningham, R. J. Beaver, and R. C. Waugh, Fuel Dispersion in Stainless Steel Components for Power Reactors, Paris Fuel Elements Conference, TID-7546, pp. 243-268 (March 1958).

8. R. H. Selner and R. L. Irwin, Ultrasonic Inspection of BORAX-V Superheater Fuel Plates, ANL-6726 (to be published).

9. N. S. Beyer, R. B. Perry, and B. F. Geren, Nondestructive Analysis by Radiation Detection of Fuel Content, Fuel Homogeneity, and Surface Contamination of the Superheater Plates for the BORAX-V Reactor, ANL-6746 (to be published).

10. ASTM Standard A393-55T, Tentative Recommended Procedure for Conducting Acidified Copper Sulfate Test for Intergranular Attack in Austenitic Stainless Steel, ASTM Standards, pp. 393-398, Part 3 (1961).

11. S. V. Smith, Shaper Scalps Stainless Steel, American Machinist/ Metalworking Manufacturing, p. 84 (Feb 5, 1962).

12. J. L. Marley and C. J. Kiley, Determination of Uranium in Stainless Steel Electrolytic-Volumetric, KAPL-M-JLM-1 (1956).

13. Statistics - A New Approach, W. Allen Wallis and Harry V. Roberts, The Free Press, Glencoe, Illinois (1958).

14. Private Communication with J. R. Cunningham and R. J. Beaver, Oak Ridge National Laboratory, February 15, 1961.

15. J. H. Cherubini, R. J. Beaver, and C. F. Leitten, Jr., Fabrication Development of UO_2-Stainless Steel Composite Fuel Plates for Core B of the Enrico Fermi Fast Breeder Reactor, ORNL-3077 (April 18, 1961).

16. G. G. Gaul, W. L. Pearl, and M. Siegler, Stress Corrosion of Type 304 SS in Simulated Superheat Reactor Environments, GEAP-4025 (Sept 26, 1962).

17. W. E. Ruther and S. Greenberg, Corrosion of Steels and Nickel Alloys in Superheated Steam, J. Electrochem. Soc., to be published.

APPENDIX A

Material Processing Contract 31-109-38-1252, Appendix B, and

Supplemental Agreement No. 1

APPENDIX B

SCOPE OF WORK

Subcontract 31-109-38-1252

The Contractor shall be responsible for converting the U_3O_8 to be supplied by the Laboratory under Paragraph 1 of Article II of this contract to UO_2 meeting the specifications set forth in Item 7 of this Appendix B.

The Contractor shall fabricate and deliver to Argonne National Laboratory, F.O.B. the Contractor's plant, 1,048 stainless steel-UO_2 plates clad with stainless steel. Two hundred eight of these plates shall consist of depleted or normal UO_2 dispersed in a stainless steel matrix, and the remaining 840 plates shall consist of highly enriched UO_2 dispersed in a stainless steel matrix. All plates shall be fabricated in accordance with the following specifications and drawing BX5-1-113-C, which is attached hereto and made a part of this contract.

1. The following quantities of plates containing the indicated weights of UO_2 will be required:

Plate Type	Quantity	UO_2 content in grams ±1 per cent
Depleted (0.22%) or normal		
HCD	52	18.3
FCD	52	34.1
HPD	52	28.9
FPD	52	54.0
Enriched (93%)		
HCE	190	18.3
FCE	190	34.1
HPE	230	28.9
FPE	230	54.0

2. The Contractor shall fabricate 12 each of plates type HCD, FCD, HPD, and FPD prior to the production of the remaining depleted or normal plates or the enriched plates. These plates shall be fabricated on the same equipment and by the identical procedures which will be used for the fabrication of the remaining depleted or normal and enriched plates. Six each of these plates will be examined by the Contractor by destructive and nondestructive testing as outlined in Items 15 and 16.

3. Plate dimensions shall be as follows:

Length	Width	Thickness
Core		
24.000" ± 0.750"	3.495" ± 0.052"	0.014" ± 0.001"
Clad Plate		
25.250" ± 0.005"	3.665" ± 0.002"	0.030" ± 0.001"

The finished plates shall be square and straight within 0.002" TIR. All four corners shall be sharp and all edges shall be sharp and free of burrs. The core shall be located symmetrically within the cladding. Based on the above dimensions, the cladding dimensions shall be as follows:

Face cladding	0.007" minimum
Side cladding	0.085" ±0.025"
End cladding	0.250" minimum

4. All finished plates shall be such that no points within two inches of each other shall vary by more than 0.002" TIR from true flatness as measured with side edges clamped to a surface plate.

5. All finished pieces shall be bright annealed to flatten the plates and to assure that no distortion will occur during subsequent heating to temperatures up to 1150°C.

6. All finished plates shall have a surface finish of 32 micro inches or better. This finish shall be so generated in the fabrication process that additional operations to improve the surface, such as grinding, machining, abrasive grit blasting, pickling, or etching, are not required. All plates shall be clean and free from radioactive surface contamination, oxide discoloration, scale, inclusions and any detectable chloride or fluorine contamination. Any cleaning or pickling solution used to remove surface contamination shall not contain any halide ion or be reducing in nature. Halides may not be used in any processing step for the steel. Surface indentations, pits, or scratches deeper than 0.001" or visible blisters shall be cause for rejection.

7. The uranium oxide shall contain a minimum of 87.8 weight per cent uranium and the impurity content shall not exceed the following amounts:

Al	100 ppm	Ca	100 ppm	Fe	300 ppm	P	100 ppm
Ag	1	Cd	0.3	K	20	Si	100
B	0.5	Co	10	Mg	10	Sn	10
Ba	10	Cr	75	Mn	10	V	25
Be	10	Cu	20	Na	20	Total	
C	100	F	200	Ni	225	Rare earths	3

The uranium dioxide powder shall be of a high-fired type with a density of 10.33 g/cc (as determined by pycnometer measurements) and shall have a particle size between 37 and 88 microns with the larger fraction at the smaller size range being most desirable.

8. The matrix material shall be AISI type 304B stainless steel powder having a maximum carbon content of 0.03 weight per cent and a silicon content of approximately 2.5 weight per cent.

9. The cladding components shall be fabricated of a suitable clad of AISI type 304L wrought stainless steel containing less than 0.05 per cent cobalt and less than 10 ppm of boron. Representative samples of each lot or billet of steel used in the fabrication of plates shall be furnished to the Laboratory for evaluation.

10. The distribution of uranium within the core of each plate shall be uniform for any core volume 1" square by core thickness to within ±2 per cent of the uranium composition of any other sample from the same core.

11. The UO_2 should be present as discrete particles within the stainless steel matrix. Fragmentation, agglomeration, and stringering of the particles shall be avoided in the fabrication process. Stringers shall be no greater than 0.01" in length. The stainless steel matrix shall be completely bonded and free of voids.

12. The core must be integrally bonded to the cladding material at all mating surfaces. This bond shall be complete to a minimum of 99.5 per cent of the interfacial area. No defect greater than 1/32" in any dimension shall be present in the bond; and no two such defects shall be within 1/2" of each other.

13. All cladding mating surfaces must be integrally bonded to each other. The bonds shall be free of contamination which might lower the corrosion resistance of the base material and be free of uranium. Any inclusion or void will be cause for rejection. If the picture frame type of billet is used in the fabrication, the frame shall be a single unit.

14. The amount and type of any material added to the core compact as binders or to facilitate sintering shall be subject to approval by the Laboratory.

15. The Contractor shall perform the following destructive tests on six each of the depleted or normal plates described in Item 1 above and on 2 per cent of all finished types HCE, FCE, HPE, and FPE fuel plates as selected at random by the Laboratory. These tests may be witnessed by ANL representatives. Selection of fuel plates to be tested shall be made after a suitable number have been received at the Laboratory.

(a) Sensitization

Sensitization to carbide precipitation may result from an increase in the carbon content of the cladding material. Any external carbon contamination shall be evaluated by testing samples taken from the plate end-cladding which does not contain oxide core material. Two 1/4" wide by 1" long specimens shall be cut from each plate, one from each end, and subjected to the Strauss Test. These tested samples shall not exhibit any evidence of cracking after bending 180° around a 1/8" diameter mandrel nor show any evidence of intergranular attack when examined metallographically at 100X in the as-polished condition.

(b) Homogeneity of Core

A total of five 1" square plate samples shall be taken from locations selected by ANL for determining homogeneity of the oxide in the plate core. These samples shall be chemically analyzed for total uranium content and the results expressed on a weight-percent basis. The allowable variation from a true uniform dispersion of uranium oxide between any two samples shall be ±2 per cent.

(c) Bond integrity

The integrity of all bond interfaces shall be determined by the examination of transverse plate sections. Minimum 1/2" wide transverse sections shall be taken at five locations selected by ANL along the plate length and two 2" long longitudinal sections selected by ANL from each end of the plate. After proper metallographic preparation and electrolytic etching with 5 per cent chromic acid reagent, these samples shall show no evidence of inclusions or lack of bond at all mating surfaces upon metallographic examination at 100X.

(d) Cladding thickness measurements

The transverse and longitudinal specimens examined in (c) above shall be used for measuring cladding thickness. The face cladding-to-core thickness on all specimens shall be measured at 1/4" intervals with a filar micrometer. A filar micrometer or optical

comparator shall be used to measure the width of the side cladding at both ends of each transverse specimen. Measurement of end cladding from the longitudinal specimens shall be made to the nearest 1/64". The cladding measurement on all samples shall be within specified tolerances.

(e) Oxide fragmentation and stringering

One longitudinal sample at least 1/2" long shall be taken from the core of each sectioned plate and examined metallographically for distribution of uranium oxide in the stainless steel matrix. These samples as viewed at 250X shall be free from voids, fragmentation, and clusters or continuous nonsegmented strings of UO_2. No stringers greater than 0.01" in length will be acceptable.

16. The Contractor shall conduct nondestructive tests on all plates. These tests may be witnessed by an ANL representative.

(a) Dimensions

All plates shall be measured for width, thickness, length, squareness, and flatness. Measurements of plate thickness shall be made at both ends of the core and at two equally spaced intervals between the ends of the core. At each of these four locations along the plate length, three thickness measurements shall be taken in line, normal to the plate longitudinal axis, one at the plate centerline, and one at each side of the plate core. A total of twelve thickness measurements shall be made and recorded. Width measurements shall also be made at four equal intervals along the plate length and recorded. Flatness measurements shall be obtained as designated in Item 4 above. All dimensions shall comply with specified tolerances, Item 3 above.

(b) Weight

All finished plates shall be weighed to within 0.1 grams.

(c) Radiograph

All finished plates shall be radiographed to show core location with respect to the ends and sides of the plate and distribution of oxide. From these radiographs, the widths of side cladding shall be measured at a minimum of three locations along each side to determine the maximum and minimum width of cladding and at two locations at each end of the plate to determine maximum and minimum end cladding length. The radiographs and record of measurements shall be delivered to ANL. Radiographs shall be identified with the plate number and bear a fiducial mark for orientation with respect to the plate.

(d) Radioactive surface contamination

All preliminary plates which are not sectioned for destructive testing shall be examined for surface contamination from radioactive substances. Inspection for alpha contamination by direct counting methods as opposed to indirect methods such as a smear test shall show no evidence of contamination.

17. Argonne National Laboratory will perform the following nondestructive tests on all plates delivered by the Contractor:

(a) Measurement for total U-235
(b) Distribution of U-235
(c) Clad thickness determination
(d) Bond integrity
(e) Radioactive surface contamination
(f) Halide ion contamination

18. The following data for each plate supplied shall be recorded and furnished in triplicate to Argonne National Laboratory:

(a) Plate number
(b) Type of plate
(c) Batch number of uranium dioxide used
(d) Weight of uranium dioxide, uranium and U-235 in finished plate
(e) Batch number of 304B stainless steel powder
(f) Weight of 304B stainless steel powder in core
(g) Maximum and minimum over-all thickness, width, and length
(h) Maximum and minimum thickness of face cladding, of width, of side cladding, and length of end cladding for each face, side, or end of the plate.
(i) Deviation from flatness, straightness, and squareness
(j) Total weight of plate

19. A complete record of all fabricating steps shall be maintained for each plate fabricated.

20. Copies of all records obtained from inspection and test results are to be provided to the Laboratory.

21. All finished plates are to contain permanent identification in the form of numbers and letters 1/16" in height stamped into the metal located near one end of the plate in the end-cladding area, not less than 1/8" from the plate core.

(a) Core length

Fuel plates having an over-all core length in excess of 24" shall be marked at one end with a plus sign inside a circle. All plates having an over-all core length of less than 24" shall be marked at one end with a minus sign inside a circle.

(b) Plate numbering

All plates shall be numbered consecutively in the order of their fabrication followed by a suffix designating the type of plate as specified in Item 1.

22. Two stainless steel coupons, one cut from each end of each plate, shall be supplied from all plates fabricated. These coupons, 1/4" by plate width, are to be cut from the plate ends before the plates are cut to final length. All coupons are to be marked with a permanent identification corresponding to the identification marking on the plate itself, (see Item 21).

23. Certified analyses for the following elements for each lot of stainless steel used for cladding components shall be furnished to the Laboratory:

C	Si	B	N
Mn	Cr	Co	Pb
P	Ni	Cu	Sn
S	Al	Mo	Ta

ARGONNE NATIONAL LABORATORY
Argonne, Illinois

Supplemental Agreement No. 1
Material Processing Contract
No. 31-109-38-1252

Argonne National Laboratory, (called the "Laboratory") operated by The University of Chicago, an Illinois not-for-profit corporation acting under Contract No. W-31-109-Eng-38 with the United States Government (called the "Government"), represented by the U. S. Atomic Energy Commission (called the "Commission") and NORTH AMERICAN AVIATION, INC., acting through its ATOMICS INTERNATIONAL DIVISION, (called the "Contractor"), a Delaware corporation, having entered into Material Processing Contract No. 31-109-38-1252, dated October 3, 1960 (called the Contract) to perform certain work under the Laboratory's prime contract, have mutually agreed to modify such Contract as hereinafter appears. Such modification is made with the understanding that the Contractor will attempt to improve its fabrication process by screening all stainless steel powder and Uranium

DWG. No. BX5-1-113-C

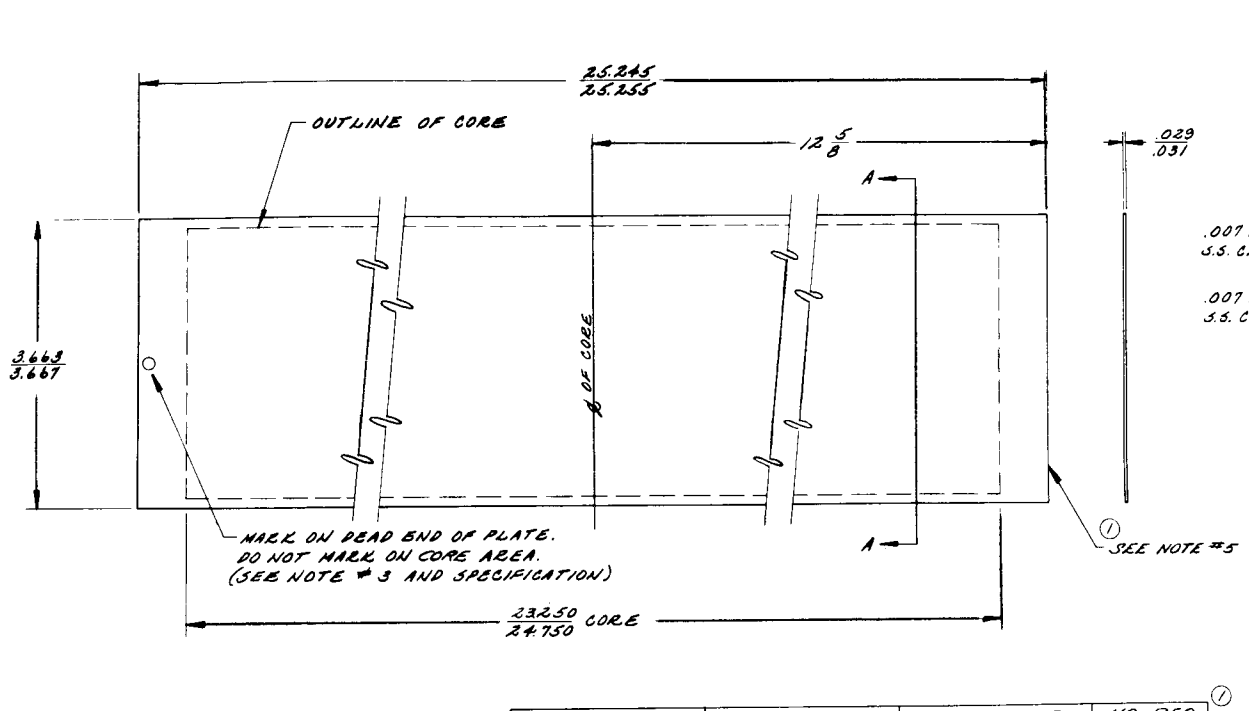

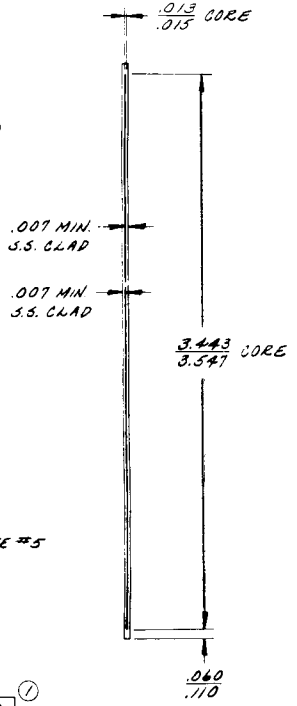

SECTION A-A
DOUBLE SCALE

NOTE:
1. PLATE TO BE SQUARE & TRUE WITHIN .002 T.I.R.
2. NO POINTS WITHIN 2" OF EACH OTHER CAN VARY BY MORE THAN .002 T.I.R. FROM TRUE FLAT, AS MEASURED WITH SIDE EDGES CLAMPED TO AN ACCURATE SURFACE PLATE.
3. PLATES WITH CORE LENGTH OVER 24" MARK WITH ⊕ (CIRCLED PLUS SIGN). PLATES WITH CORE LENGTH UNDER 24" MARK WITH ⊖ (CIRCLED MINUS SIGN). LOADING OF FUEL PLATES SHALL BE INDICATED BY LETTERS.
1 4. FINISH ALL OVER 32
5. BREAK EDGES ON ENDS OF PLATE ONLY, .005 TO .010 OR FORM FULL .015 RADIUS. (TO BE DONE BY A.N.L.)

1

PART NO.	TYPE FUEL PLATE	NEXT ASSEMBLY	NO. REQ.
BX5-1-113-C(FCE)	CENTRAL	BX5-1-449-D(C)	2
	FULL LOAD	BX5-1-296-D	1
BX5-1-113-C(HCE)	CENTRAL	BX5-1-449-D(C)	2
	HALF LOAD	BX5-1-296-D	1
BX5-1-113-C(FPE)	PERIPHERAL	BX5-1-449-D(P)	2
	FULL LOAD	BX5-1-296-D	1
BX5-1-113-C(HPE)	PERIPHERAL	BX5-1-449-D(P)	2
	HALF LOAD	BX5-1-296-D	1

						SEE TABLE	SEE TABLE
						NEXT ASSEMBLY	NO. REQUIRED
						ARGONNE NATIONAL LABORATORY	
						THIS DRAWING IS THE PROPERTY OF THE ARGONNE NATIONAL LABORATORY	
						TITLE PLATE-ELEMENT FUEL-MOD. 4-BORAX II	
1		ADDED NOTE #5 & TABLE	11/62	T.J.	AWC	SCALE FULL	DWG. NO. BX5-1-113-C
STYL	ZONE	CHANGE	DATE	BY	CH'K		

RECORD-FILE STAMP

APPROVED CHIEF ENGR. — DATE 9/11/62
STAFF APPROVAL REPRESENTATIVE — DATE 11/8/62
CHIEF DRAFTSMAN — DATE
CHECKED — DATE 3/27/63
SCALE 12 — DRAWN BY — DATE 3/26/63

TOLERANCES UNLESS OTHERWISE NOTED
FRACTIONAL ± 1/64 DECIMAL ± .005 ANGLE ± 1/4°
REMOVE ALL BURRS

MATERIAL CORE - U.S. 304S # UO_2
CLAD - S.S. 304L

Dioxide powder to insure proper powder size and by making such other changes in its fabrication process as Contractor may consider beneficial in the performance of work hereunder.

Therefore, the parties mutually agree as follows:

1. (a) Article III is amended to delete the clause reading "The Contractor agrees to make delivery as follows:"

   (b) Paragraph 1 of Article III is deleted and the following substituted in lieu thereof:

   "Contractor, having delivered six (6) each of plates type HCD, FCD, HPD and FPD to the Laboratory for testing, and the HCD and FPD type plates having met the specifications hereunder, as amended by Supplemental Agreement No. 1 to this contract, the Contractor agrees to exert its best efforts to deliver to the Laboratory, within two and one-half weeks after the date of Supplemental Agreement No. 1 to this contract an additional six (6) each of plates FCD and HPD for evaluation."

   (c) Paragraph 2 of Article III is deleted and the following substituted in lieu thereof:

   "Contractor, having furnished to the Laboratory the test data required by Appendix B concerning the examination by the Contractor of six (6) each of plates type HCD and FPD, agrees to furnish to the Laboratory such test data concerning Contractor examination of four (4) each of plates type FCD and HPD within two weeks after delivery of such type plates to the Laboratory in accordance with paragraph 1 of this Article III."

2. Paragraph 3 of Article III is deleted and the following substituted in lieu thereof:

   "One thousand (1,000) plates consisting of forty (40) each of types HCD, FCD, HPD, and FPD, one hundred-ninety (190) each of types HCE and FCE, and two hundred-thirty (230) each of types HPE and FPE shall be delivered by the Contractor to a carrier, f.o.b., Canoga Park, California, for shipment to Argonne National Laboratory, Argonne, Illinois, in accordance with the following schedule:

   Forty (40) each of plates HCD and FCD within four (4) weeks after the date of Supplemental Agreement No. 1 to this contract.

   One hundred-ninety (190) each of plates HCE and FCE within ten (10) weeks after the date of Supplemental Agreement No. 1 to this contract.

Forty (40) each of plates HPD and FPD within twelve (12) weeks after the date of Supplemental Agreement No. 1 to this contract.

Two hundred thirty (230) each of plates HPE and FPE within twenty (20) weeks after the date of Supplemental Agreement No. 1 to this contract.

3. Paragraphs 1 and 2 of Article IV - PRICE AND PAYMENT are deleted and the following substituted in lieu thereof:

"1. The total price for the performance of all work provided for herein is one hundred fifty-six thousand, one hundred twenty-five dollars ($156,125.00).

2. Payment shall go forward as follows:

(a) Sixty two thousand, four hundred fifty dollars ($62,450) shall be due and payable upon approval by the Laboratory of the HCD and FPD plates delivered as stated in paragraph 1 of Article III above.

(b) Sixty two thousand, four hundred fifty dollars ($62,450) shall be due and payable on receipt by the Laboratory of the plates to be delivered under paragraph 3 of Article III above at the rate of Sixty two dollars and forty-five cents ($62.45) per plate.

(c) Thirty one thousand, two hundred twenty five dollars ($31,225.00) shall be due and payable ninety (90) days after receipt by the Laboratory of all the plates to be delivered under this contract."

4. Appendix B, SCOPE OF WORK, is amended as follows:

(a) The second paragraph on page 1 shall be amended as follows:

(1) In the first sentence, the figures "1,048" shall be deleted and the figures "1,044" shall be substituted in lieu thereof.

(2) In the second sentence, the words "Two hundred eight" shall be deleted and the words "Two hundred four" shall be substituted in lieu thereof.

(b) In paragraph 1, change the quantity of plate types FCD and HPD from "52" to "50."

(c) In paragraph 11, change "0.01" to "0.02."

(d) In paragraph 15, delete the first sentence and substitute in lieu thereof the following:

"The Contractor shall perform the following destructive tests on four (4) each of plate types FCE and HPD and on 2% of all finished plates types HCE, FCE, HPE, and FPE as selected at random by the Laboratory, except that the Laboratory shall perform the chemical analyses for UO_2 required in connection with these tests on finished plates types HCE, FCE, HPE, and FPE."

(e) In subparagraph (b) of paragraph 15, change "±2" to "±5."

(f) In subparagraph (e) of paragraph 15, change "0.01" to "0.02."

5. All other terms and conditions of the Contract shall remain in full force and effect.

IN WITNESS WHEREOF, the parties hereto have executed this Supplemental Agreement this 22nd day of June, 1961.

ARGONNE NATIONAL LABORATORY
(Operated by The University of Chicago)

By _____
J. H. McKinley
Title Business Manager

NORTH AMERICAN AVIATION, INC.

By _____
J. J. Flaherty
Title Executive Vice President
Atomics International Division

I, E. N. Yost, certify that I am an Assistant Secretary of the corporation named as the "Contractor" in the within Supplemental Agreement; that J. J. Flaherty who signed the said Supplemental Agreement on behalf of the Contractor was the Exec. Vice Pres., Atomics International Div. of said corporation, that I know his signature and his signature thereto is genuine; and that said Supplemental Agreement was duly signed, sealed and attested for and in behalf of said corporation by authority of its governing body.

By _____
E. N. Yost
Title Assistant Secretary

APPENDIX B

Calculation of the Standard Deviation of Sample Values

X = a sample value.

N = the total number of sample values taken.

$\overline{X}$ = the mean of N sample values.

$$S = \sqrt{\frac{\Sigma (X - \overline{X})^2}{N}},$$

where S is the standard deviation of all sample values taken.

$\overline{X} \pm 2S$ = the range within which 95% of the N sample values fall.

σ (sigma) = the true standard deviation of the universe from which the N sample values were taken.

$\overline{A}$ = the true mean of all measurable values within the universe from which the N sample values were taken.

$\overline{A} \pm 2\sigma$ = the true range which includes 95% of all universe sample values.

$\overline{X} \pm 2S$ is, then, an approximation of the actual 2σ (2 sigma) range, $\overline{A} \pm 2\sigma$.

LEGAL NOTICE

This report was prepared as an account of Government sponsored work. Neither the United States, nor the Commission, nor any person acting on behalf of the Commission:

A. Makes any warranty or representation, expressed or implied, with respect to the accuracy, completeness, or usefulness of the information contained in this report, or that the use of any information, apparatus, method, or process disclosed in this report may not infringe privately owned rights; or

B. Assumes any liabilities with respect to the use of, or for damages resulting from the use of any information, apparatus, method, or process disclosed in this report.

As used in the above, "person acting on behalf of the Commission" includes any employee or contractor of the Commission, or employee of such contractor, to the extent that such employee or contractor of the Commission, or employee of such contractor prepares, disseminates, or provides access to, any information pursuant to his employment or contract with the Commission, or his employment with such contractor.

Price $1.75 . *Available from the Office of Technical Services, Department of Commerce, Washington 25, D.C.*